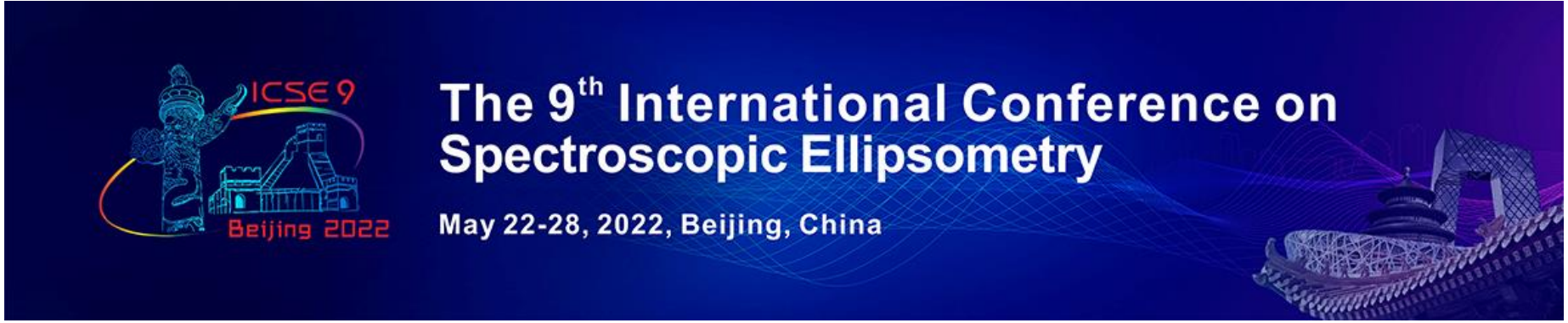

Exploring the sensitivity limits of a Mueller matrix ellipsometer.
The spatial dispersion of Si

Oriol Arteaga

UNIVERSITAT DE BARCELONA

Preface

Ellipsometry is on most occasions regarded as a “very sensitive” optical technique

This sensitivity is usually referring to its capacity to detect *small changes in the thickness of thin films*

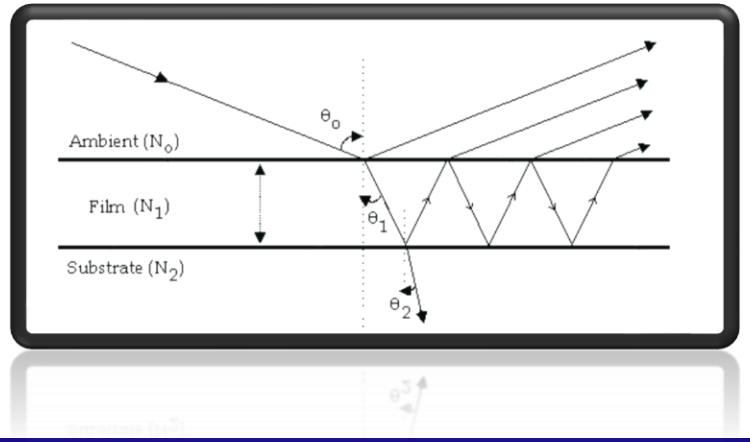

Preface

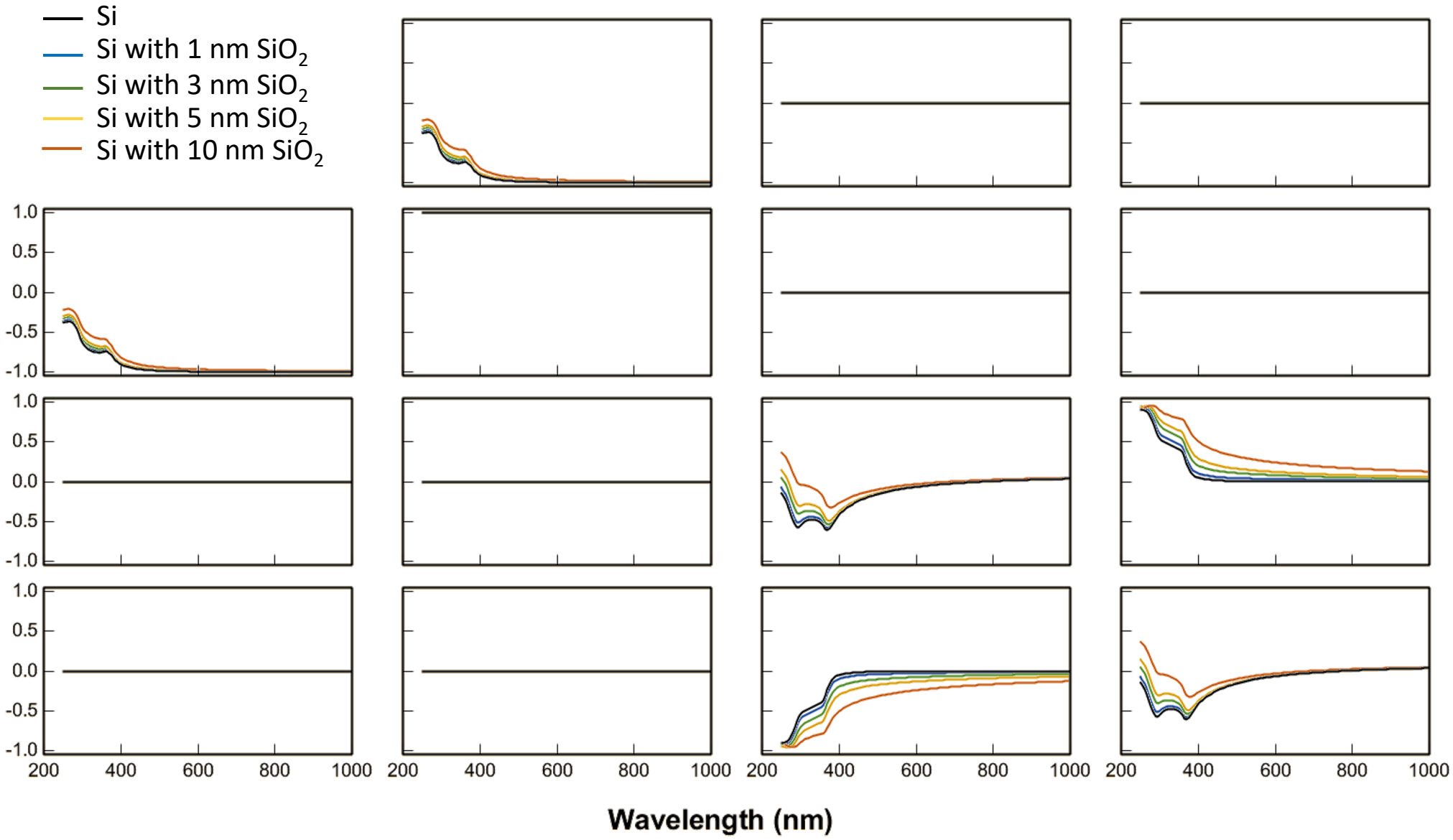
Si
Si with 1 nm SiO2
Si with 3 nm SiO2
Si with 5 nm SiO2
Si with 10 nm SiO2
1.0
0.5
0.0
-0.5
-1.0
200
400
600
800
1000
Wavelength (nm)

Preface

Of course, this is far from being new

1850 Jules Jamin

(263)

MÉMOIRE SUR LA RÉFLEXION A LA SURFACE DES CORPS TRANSPARENTS;

PAR M. J. JAMIN.

De tous les problèmes d'optique, celui qu
d'hui le mieux résolu est sans contredit
flexion : les phénomènes, toujours conform
mathématiques, ont été si souvent prévus p
nouvelles expériences sur cette matière par
flues, si quelques objections graves qu'on r
reproduire ne laissaient quelque doute dan

observe les mêmes variations de teinte. Il est impossible de conserver des doutes sur la signification théorique de ces expériences ; elles se résument ainsi :

1°. Les substances transparentes ne polarisent pas complétement la lumière.

2°. Elles transforment la polarisation rectiligne d'un faisceau incident en une polarisation elliptique.

3°. La différence de marche des rayons principaux éprouve les mêmes variations que pour les métaux entre les incidences limites.

Au point de vue théorique, ces conclusions ont une grande importance; nous montrerons bientôt cependant que les formules de Fresnel expriment avec une approximation pratique suffisante les intensités de la lumière réfléchie: mais nous voyons dès maintenant qu'elles ne prévoient aucunement un des phénomènes les plus importants de la réflexion, celui du changement des phases; dès lors elles perdent leur caractère de généralité, et cessent d'être l'expression rationnelle des phénomènes. Nous nous occuperons dans la suite des expressions théoriques qui doivent

Ellipsometry was so sensitive to the overlayers, that Jamin found he could not fully verify Fresnel's equations

Jamin's ellipsometer design with a Senármont compensator, was already commercial during the XIX century!

Preface

THE REVIEW OF SCIENTIFIC INSTRUMENTS VOLUME 16, NUMBER 2 FEBRUARY, 1945

The Ellipsometer, an Apparatus to Measure Thicknesses of Thin Surface Films

ALEXANDRE ROTHEN
Laboratories of The Rockefeller Institute for Medical Research, New York, New York

(Received October 9, 1944)

An apparatus designed to determine the thickness of films deposited on metal slides is described. It is based on the measurement of the change that takes place in ellipticity of the light reflected after a slide has been coated with the film under investigation. The apparatus is capable of measuring a film thickness within ±0.3A, a sensitivity at least ten times greater than that obtained with the method based on light interference.

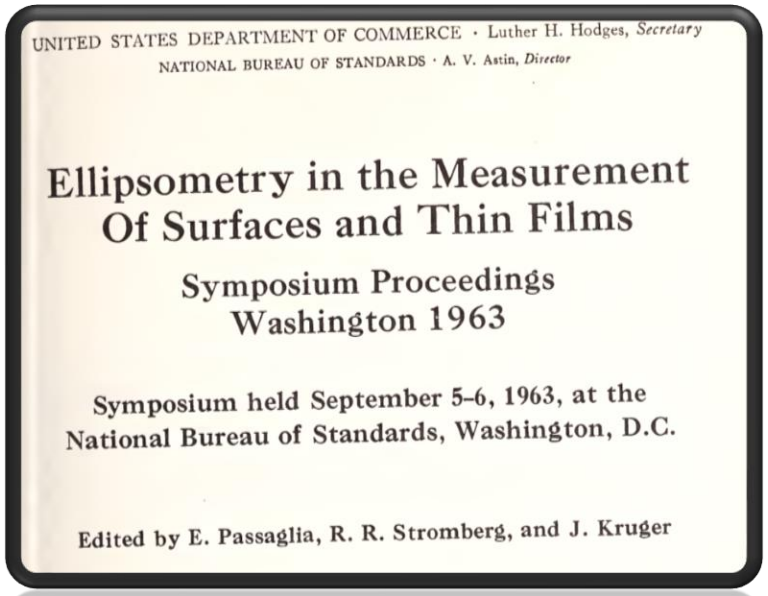

UNITED STATES DEPARTMENT OF COMMERCE · Luther H. Hodges, *Secretary*
NATIONAL BUREAU OF STANDARDS · A. V. Astin, *Director*

Ellipsometry in the Measurement Of Surfaces and Thin Films

Symposium Proceedings
Washington 1963

Symposium held September 5-6, 1963, at the National Bureau of Standards, Washington, D.C.

Edited by E. Passaglia, R. R. Stromberg, and J. Kruger

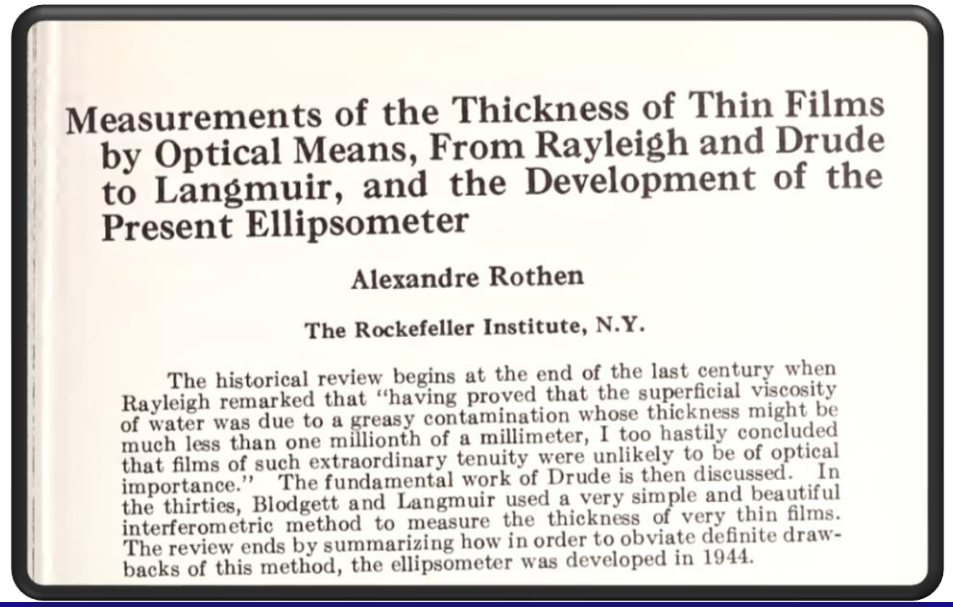

Measurements of the Thickness of Thin Films by Optical Means, From Rayleigh and Drude to Langmuir, and the Development of the Present Ellipsometer

Alexandre Rothen

The Rockefeller Institute, N.Y.

The historical review begins at the end of the last century when Rayleigh remarked that "having proved that the superficial viscosity of water was due to a greasy contamination whose thickness might be much less than one millionth of a millimeter, I too hastily concluded that films of such extraordinary tenuity were unlikely to be of optical importance." The fundamental work of Drude is then discussed. In the thirties, Blodgett and Langmuir used a very simple and beautiful interferometric method to measure the thickness of very thin films. The review ends by summarizing how in order to obviate definite drawbacks of this method, the ellipsometer was developed in 1944.

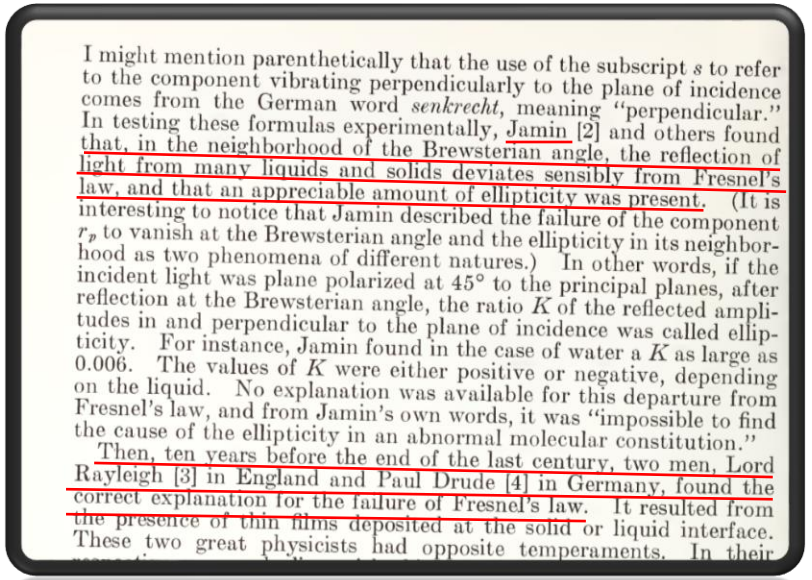

I might mention parenthetically that the use of the subscript s to refer to the component vibrating perpendicularly to the plane of incidence comes from the German word *senkrecht*, meaning "perpendicular." In testing these formulas experimentally, Jamin [2] and others found that, in the neighborhood of the Brewsterian angle, the reflection of light from many liquids and solids deviates sensibly from Fresnel's law, and that an appreciable amount of ellipticity was present. (It is interesting to notice that Jamin described the failure of the component r_p to vanish at the Brewsterian angle and the ellipticity in its neighborhood as two phenomena of different natures.) In other words, if the incident light was plane polarized at 45° to the principal planes, after reflection at the Brewsterian angle, the ratio K of the reflected amplitudes in and perpendicular to the plane of incidence was called ellipticity. For instance, Jamin found in the case of water a K as large as 0.006. The values of K were either positive or negative, depending on the liquid. No explanation was available for this departure from Fresnel's law, and from Jamin's own words, it was "impossible to find the cause of the ellipticity in an abnormal molecular constitution."

Then, ten years before the end of the last century, two men, Lord Rayleigh [3] in England and Paul Drude [4] in Germany, found the correct explanation for the failure of Fresnel's law. It resulted from the presence of thin films deposited at the solid or liquid interface. These two great physicists had opposite temperaments. In their

Preface

But in other types of measurements ellipsometry is not *intrinsically* so sensitive

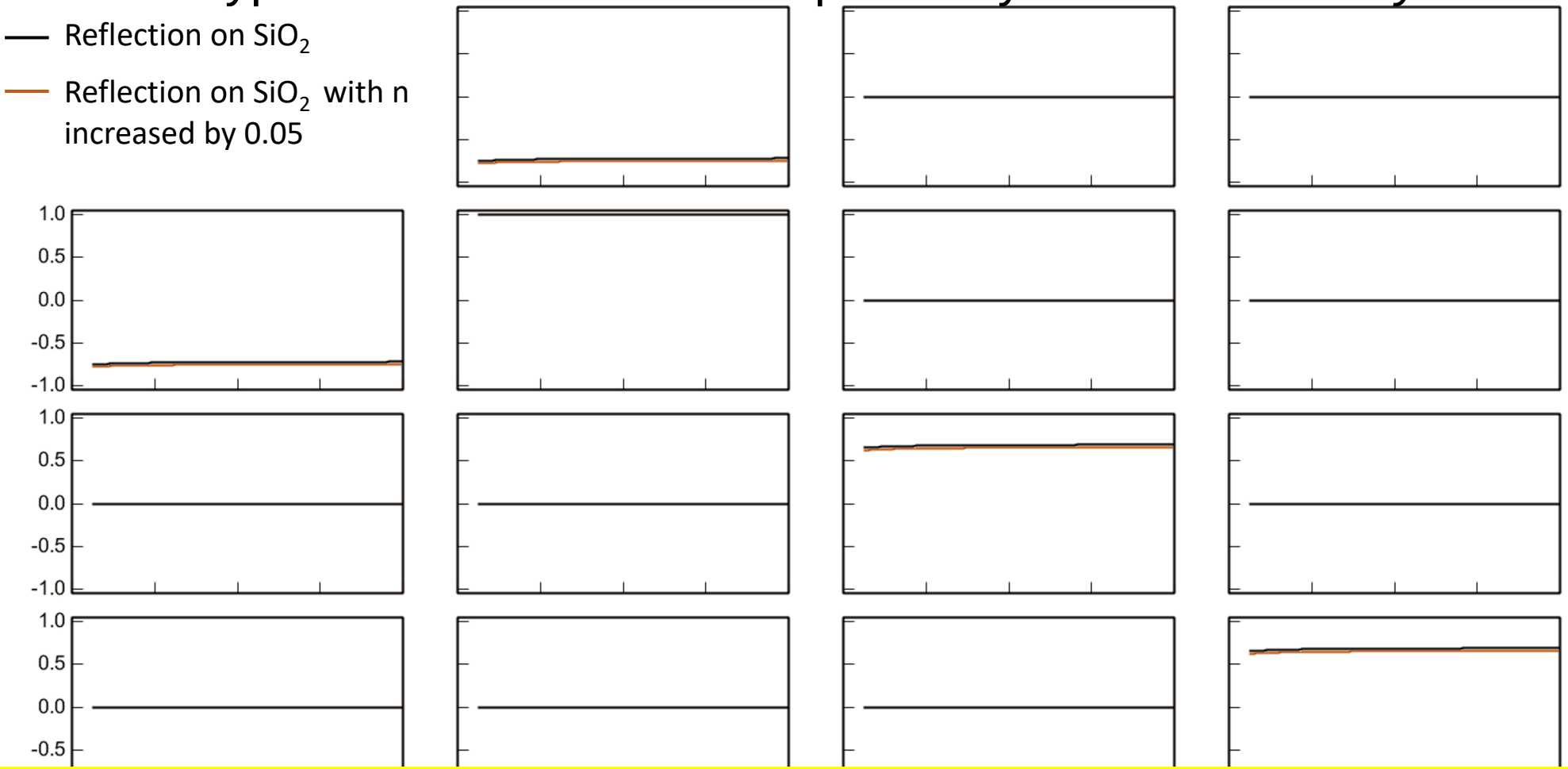

Many applications of ellipsometry demand highly sensitive instruments: optical constants, anisotropy, optical activity…

Outline

1. From intensities to Mueller matrices

2. Optimizing a dual rotating compensator MM ellipsometer

3. Optimizing a 4-photoelastic modulator MM ellipsometer

4. Spatial dispersion in Si (a challenging measurement)

1. From intensities to Mueller matrices

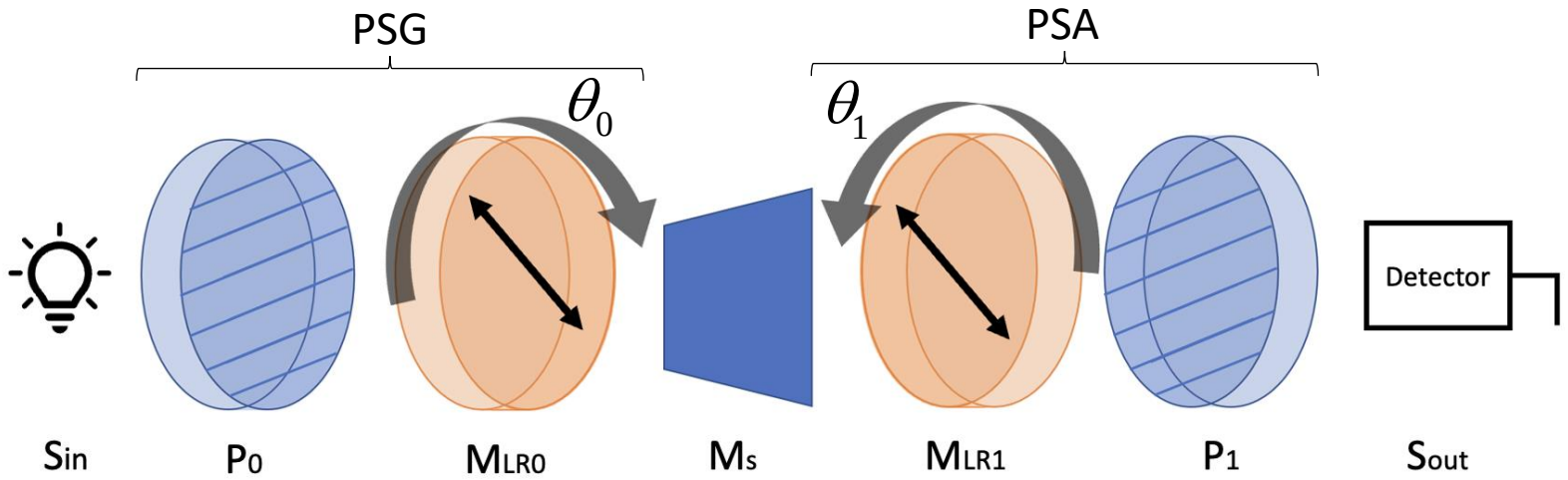

$$\mathbf{S_{out}} = \mathbf{P_1 R}(\theta_1)\mathbf{M_{LR1}R}(-\theta_1)\mathbf{MR}(\theta_0)\mathbf{M_{LR0}R}(-\theta_0)\mathbf{P_0 S_{in}}$$

PSA PSG

If only the first element of the output Stokes vector is measured

$$I_n = \underbrace{\begin{pmatrix} a_{n,0} & a_{n,1} & a_{n,2} & a_{n,3} \end{pmatrix}}_{\text{PSA}} \begin{bmatrix} m_{00} & m_{01} & m_{02} & m_{03} \\ m_{10} & m_{11} & m_{12} & m_{13} \\ m_{20} & m_{21} & m_{22} & m_{23} \\ m_{30} & m_{31} & m_{32} & m_{33} \end{bmatrix} \overbrace{\begin{bmatrix} g_{n,0} \\ g_{n,1} \\ g_{n,2} \\ g_{n,3} \end{bmatrix}}^{\text{PSG}}$$

n is the number of intensity measurements

1. From intensities to Mueller matrices

$$I_n = \begin{pmatrix} a_{n,0} & a_{n,1} & a_{n,2} & a_{n,3} \end{pmatrix} \begin{bmatrix} m_{00} & m_{01} & m_{02} & m_{03} \\ m_{10} & m_{11} & m_{12} & m_{13} \\ m_{20} & m_{21} & m_{22} & m_{23} \\ m_{30} & m_{31} & m_{32} & m_{33} \end{bmatrix} \begin{bmatrix} g_{n,0} \\ g_{n,1} \\ g_{n,2} \\ g_{n,3} \end{bmatrix}$$

n is the number of intensity measurements at the detector (usually as a function of time)

$$I_n = \mathbf{A}_n{}^T \mathbf{M} \mathbf{G}_n$$

$$\boxed{I_n = \mathbf{W}_n{}^T \cdot \vec{\mathbf{M}}}$$

$$\mathbf{W}_n = \mathbf{A}_n \otimes_{Kron} \mathbf{G}_n = \begin{bmatrix} a_0 g_0 & a_0 g_1 & a_0 g_2 & a_0 g_3 & a_1 g_0 & a_1 g_1 & a_1 g_2 & a_1 g_3 & a_2 g_0 & a_2 g_1 & a_2 g_2 & a_2 g_3 & a_3 g_0 & a_3 g_1 & a_3 g_2 & a_3 g_3 \end{bmatrix}_n^T$$

$$\vec{\mathbf{M}} = \begin{bmatrix} m_{00} & m_{01} & m_{02} & m_{03} & m_{10} & m_{11} & m_{12} & m_{13} & m_{20} & m_{21} & m_{22} & m_{23} & m_{30} & m_{31} & m_{32} & m_{33} \end{bmatrix}^T$$

1. From intensities to Mueller matrices

The n-th measurement

$$I_n = \mathbf{W}_n^T \cdot \vec{\mathbf{M}}$$

The full collection of measurements can be described by:

$$\mathbf{I} = \mathbf{W}\vec{\mathbf{M}}$$

W is a matrix of n rows and 16 columns

Data processing in an ellipsometer is the inversion of this equation

$$\vec{\mathbf{M}} = \mathbf{W}^{+}\mathbf{I}$$

$$\mathbf{W}^{+} = (\mathbf{W}^T\mathbf{W})^{-1}\mathbf{W}^T$$

Moore-Penrose pseudoinverse

Optimal (least-squares) data reduction

Applicable ALWAYS

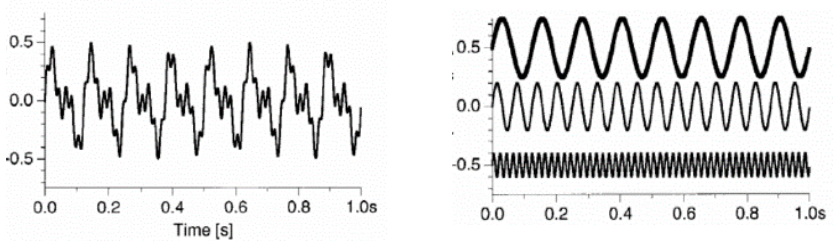

Fourier analysis of the detected signal

Mueller matrix elements calculated from Fourier coefficients

Applicable for periodic “channeled” signals

1. From intensities to Mueller matrices

Example: detected intensity for a dual rotating compensator system

As dot product

$$I_n = \mathbf{W}_n^T \cdot \vec{\mathbf{M}}$$

$$I = \begin{bmatrix} 1 \\ C_{2\theta_0}^2 + C_{\delta_0} S_{2\theta_0}^2 \\ C_{2\theta_0} S_{2\theta_0}(1 - C_{\delta_0}) \\ S_{\delta_0} S_{2\theta_0} \\ -(C_{2\theta_1}^2 + C_{\delta_1} S_{2\theta_1}^2) \\ -(C_{2\theta_0}^2 + C_{\delta_0} S_{2\theta_0}^2)(C_{2\theta_1}^2 + C_{\delta_1} S_{2\theta_1}^2) \\ -C_{2\theta_0} S_{2\theta_0}(1 - C_{\delta_0})(C_{2\theta_1}^2 + C_{\delta_1} S_{2\theta_1}^2) \\ -(S_{\delta_0} S_{2\theta_0})(C_{2\theta_1}^2 + C_{\delta_1} S_{2\theta_1}^2) \\ -C_{2\theta_1} S_{2\theta_1}(1 - C_{\delta_1}) \\ -(C_{2\theta_0}^2 + C_{\delta_0} S_{2\theta_0}^2)[C_{2\theta_1} S_{2\theta_1}(1 - C_{\delta_1})] \\ -[C_{2\theta_0} S_{2\theta_0}(1 - C_{\delta_0})][C_{2\theta_1} S_{2\theta_1}(1 - C_{\delta_1})] \\ -S_{\delta_0} S_{2\theta_0}[C_{2\theta_1} S_{2\theta_1}(1 - C_{\delta_1})] \\ S_{\delta_1} S_{2\theta_1} \\ S_{\delta_1} S_{2\theta_1}[C_{2\theta_0}^2 + C_{\delta_0} S_{2\theta_0}^2] \\ S_{\delta_1} S_{2\theta_1}[C_{2\theta_0} S_{2\theta_0}(1 - C_{\delta_0})] \\ S_{\delta_0} S_{2\theta_0} S_{\delta_1} S_{2\theta_1} \end{bmatrix}^T \begin{bmatrix} m_{00} \\ m_{01} \\ m_{02} \\ m_{03} \\ m_{10} \\ m_{11} \\ m_{12} \\ m_{13} \\ m_{20} \\ m_{21} \\ m_{22} \\ m_{23} \\ m_{30} \\ m_{31} \\ m_{32} \\ m_{33} \end{bmatrix}$$

O. Arteaga et al., "Mueller matrix microscope with a dual continuous rotating compensator setup and digital demodulation," Appl. Opt. 53, 2236-2245 (2014)

As Fourier coefficients

$$\mathcal{I} = a_0 + \sum_{n=1}^{12} (a_n \cos n\omega_f t + b_n \sin n\omega_f t),$$

Table 1. Relations between the Signal Fourier Amplitudes and the Elements of the Scaled Mueller Matrix M′

n	0	1	2	3	4	5	6
a_n	$m'_{11} + \frac{1}{2}m'_{12} + \frac{1}{2}m'_{21} + \frac{1}{4}m'_{22}$	0	$\frac{1}{2}m'_{12} + \frac{1}{4}m'_{22}$	$-\frac{1}{4}m'_{43}$	$-\frac{1}{2}m'_{44}$	0	$\frac{1}{2}m'_{44}$
b_n		$m'_{14} + \frac{1}{2}m'_{24}$	$\frac{1}{2}m'_{13} + \frac{1}{4}m'_{23}$	$-\frac{1}{4}m'_{42}$	0	$-m'_{41} - \frac{1}{2}m'_{42}$	0

n	7	8	9	10	11	12
a_n	$\frac{1}{4}m'_{43}$	$\frac{1}{8}m'_{22} + \frac{1}{8}m'_{33}$	$\frac{1}{4}m'_{34}$	$\frac{1}{2}m'_{21} + \frac{1}{4}m'_{22}$	$-\frac{1}{4}m'_{34}$	$\frac{1}{8}m'_{22} - \frac{1}{8}m'_{33}$
b_n	$-\frac{1}{4}m'_{42}$	$-\frac{1}{8}m'_{23} + \frac{1}{8}m'_{32}$	$-\frac{1}{4}m'_{24}$	$\frac{1}{2}m'_{31} + \frac{1}{4}m'_{32}$	$\frac{1}{4}m'_{24}$	$\frac{1}{8}m'_{23} + \frac{1}{8}m'_{32}$

R. M. A. Azzam, "Photopolarimetric measurement of the Mueller matrix by Fourier analysis of a single detected signal," Opt. Lett. 2, 148-150 (1978)

2. Optimizing a dual rotating compensator MM ellipsometer

$$\vec{\mathbf{M}} = \mathbf{W}^{+}\mathbf{I}$$
$$\mathbf{W}^{+} = (\mathbf{W}^{T}\mathbf{W})^{-1}\mathbf{W}^{T}$$

The optimization has been discussed in many works.
Maximize the determinant $\det(\mathbf{W}^{T}\mathbf{W})$
Minimize the condition number $\mathrm{cond}(\mathbf{W}) = \|\mathbf{W}\|\|\mathbf{W}^{+}\|$

Retardance

Optimal value $\delta \simeq 132°$

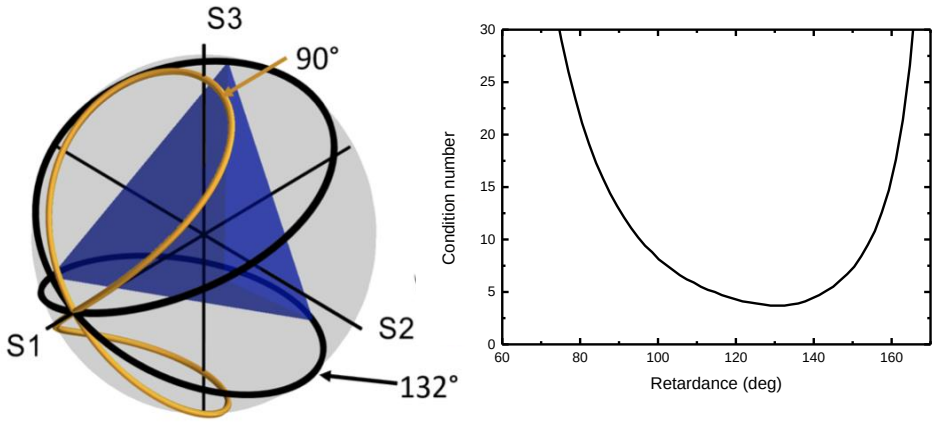

D. S. Sabatke et al. , "Optimization of retardance for a complete Stokes polarimeter," Opt. Lett. 25, 802-804 (2000)

Angles

Discrete rotation
Better for a small number of sampled intensities

Continuous rotation
(Speed ratios 5:1 or 5:3)
Better for many sampled intensities

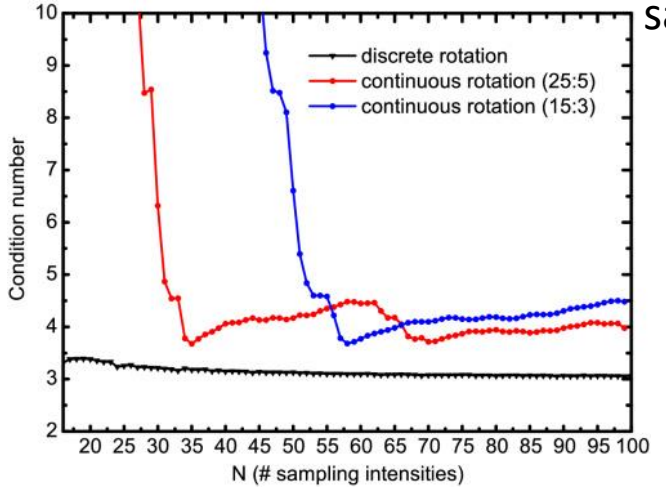

S. Bian, C. Cui, and O. Arteaga, "Mueller matrix ellipsometer based on discrete-angle rotating Fresnel rhomb compensators," Appl. Opt. 60, 4964-4971 (2021)

2. Optimizing a dual rotating compensator MM ellipsometer

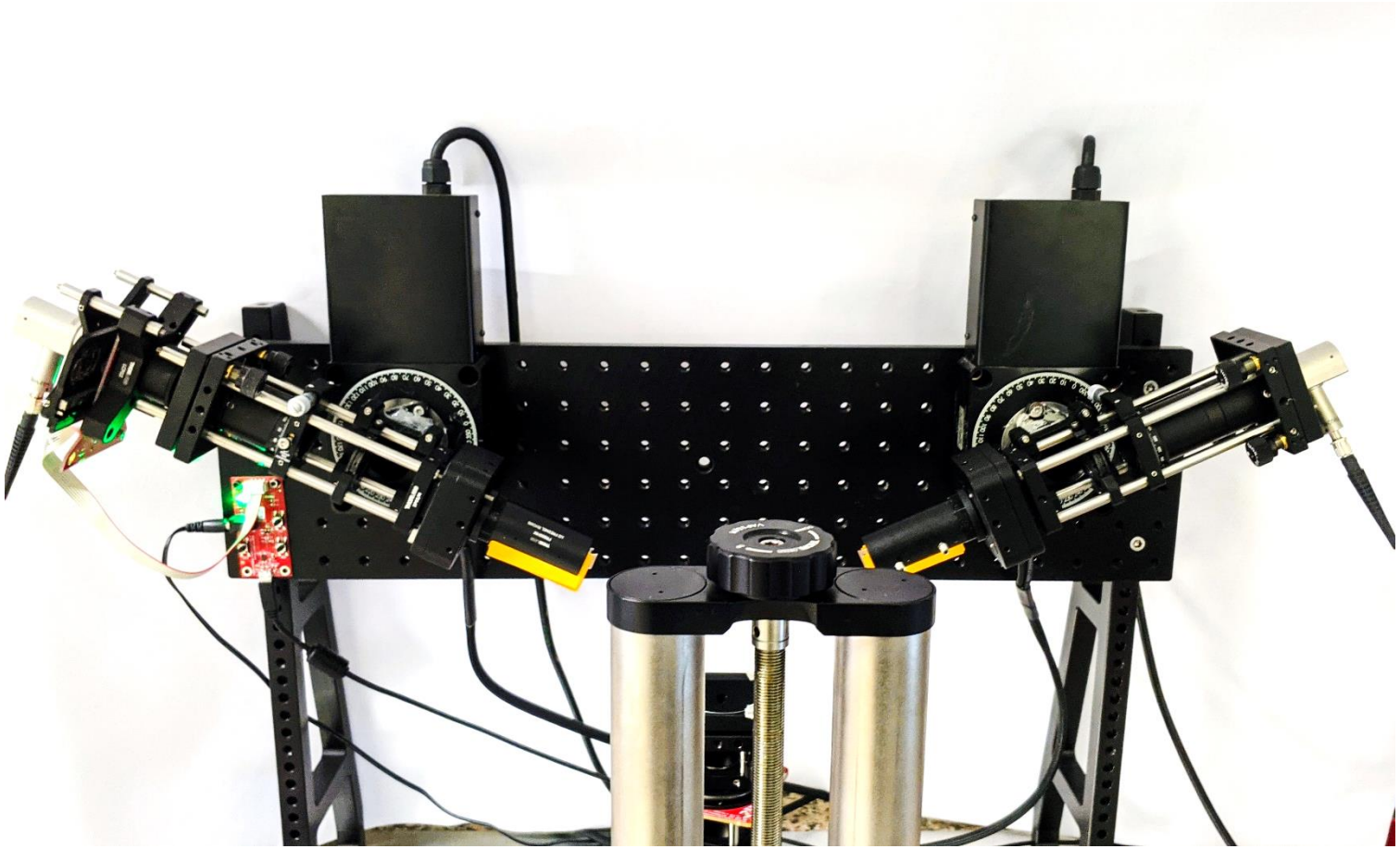

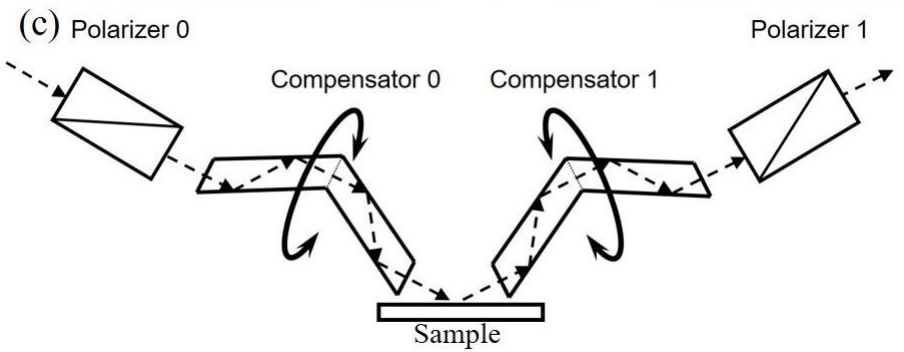

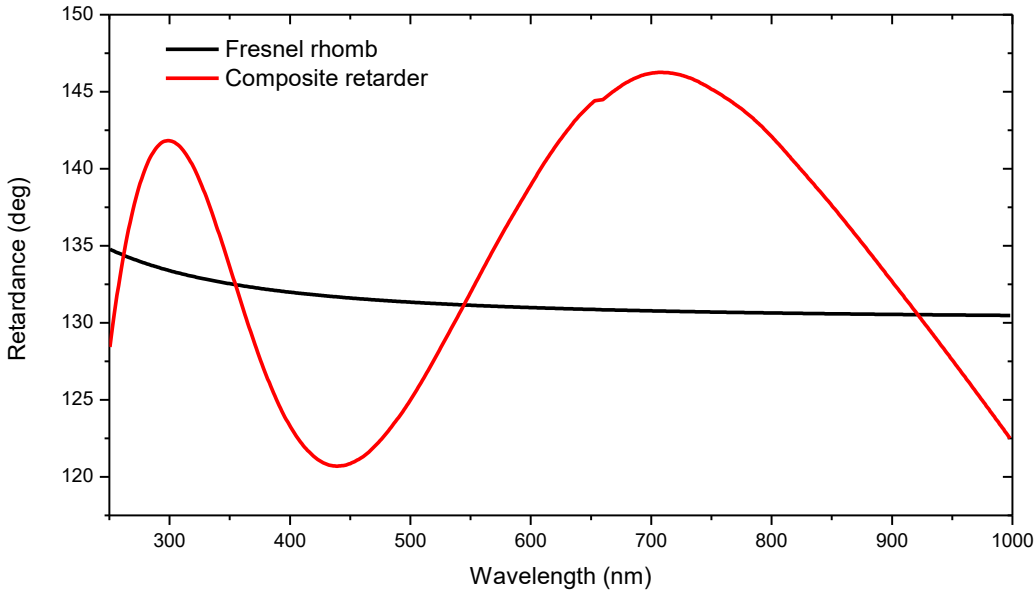

S. Bian, C. Cui, and O. Arteaga, "Mueller matrix ellipsometer based on discrete-angle rotating Fresnel rhomb compensators," Appl. Opt. 60, 4964-4971 (2021)

* Achromatic waveplate according to the design of Honggang Gu *et al* 2016 *J. Opt.* **18** 025702

2 Optimizing a dual rotating compensator MM ellipsometer

Calibration of achromatic Fresnel rhombs with an elliptical retarder model in Mueller matrix ellipsometers.

Subiao Bian[1,2], Xipeng Xu[2] and Changcai Cui[2*], Oriol Arteaga[1*]

[1]Dep. Física Aplicada, IN2UB, Universitat de Barcelona, Barcelona 08028, Spain
[2]Mechanical engineering institute, Huaqiao University, Xiamen 361021, China
E-mail :oarteaga@ub.edu cccui@hqu.edu.cn

1 INTRODUCTION

Fresnel rhombs are one of most favourable of compensating elements for spectroscopic Mueller matrix ellipsometers (MME) because they are the most achromatic form of retarders. Moreover, they can be manufactured with retardance values close to the optimal 132º value to increase the robustness of measurements. According to our observations, the small stress in the rhomb caused by the mount or produced during the fabrication can affect the ellipsometry measurements with systematic errors. This work describes a calibration method to consider this non-ideal response of the Fresnel rhomb, and that it is especially well suited for MME. The method describes each rhomb as the most general form of an elliptical retarder with a small ellipticity, instead of simply assuming that they behave as linear retarders. The results of our calibration will be illustrated by 110 plane silicon MME.

2 INSTRUMENT DESCRIPTION

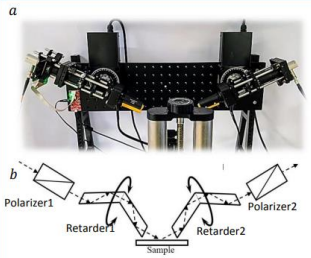

Photo (a) and scheme (b) of the MM ellipsometer based on rotating Fresnel rhomb compensators.

3 ELLIPTICAL RETARDER MODEL

$$\begin{bmatrix} 1 & 0 & 0 & 0 \\ 0 & cosT_R + LB^2\alpha & LBLB^{'}\alpha + CB\beta & -LBCB\alpha + LB^{'}\beta \\ 0 & LBLB^{'}\alpha - CB\beta & cosT_R + LB^{'2}\alpha & -LB^{'}CB\alpha^{'} - LB\beta \\ 0 & -LBCB\alpha - LB^{'}\beta & -LB^{'}CB\alpha + LB\beta & cosT_R + CB^2\alpha \end{bmatrix}$$

$$\alpha = (1 - \cos T_R)/T_R^2,\ \beta = (\sin T_R)/T_R^2$$

$$T_R = \sqrt{LB^2 + LB^{'2} + CB^2}$$

Elliptical retarder Mueller matrix, where LB, LB´ and CB represent horizontal linear birefringence projection, 45^0 linear birefringence projection and circular birefringence in experimental system coordinate.

The retardance and orientation angle of Fresnel rhomb can be respectively deduced from

$$\delta = \sqrt{LB^2 + LB^{'2}},\qquad \theta = 0.5 * \arctan(LB^{'2}/LB)$$

4 CALIBRATION OF SYSTEM PARAMETERS

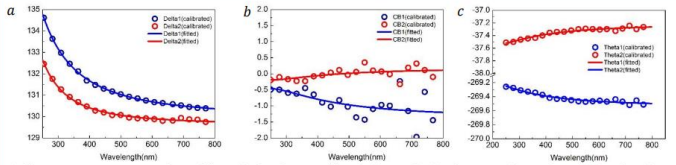

Calibration parameters: retardance (a) circular birefrigence (b) and offset angle (c), where retardance of Fresnel rhomb is close to designed value 132º, *and* circular birfrigence caused by stress is close to 0º.

5 MEASUREMENT EXAMPLES

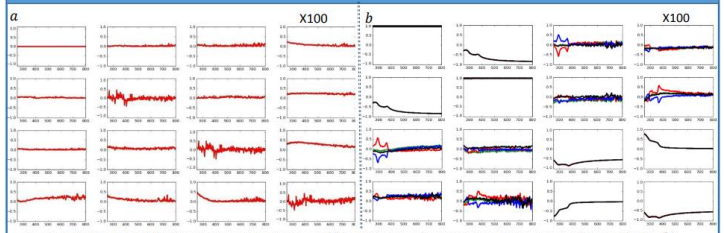

Measured air Mueller matrix with substracted identity matrix (a)and 110 plane silicon wafer mueller matrix at different azimuths (b)

Subiao Bian

Poster A36
Wed. May 25, 2022

3. Optimizing a 4-photoelastic modulator MM ellipsometer

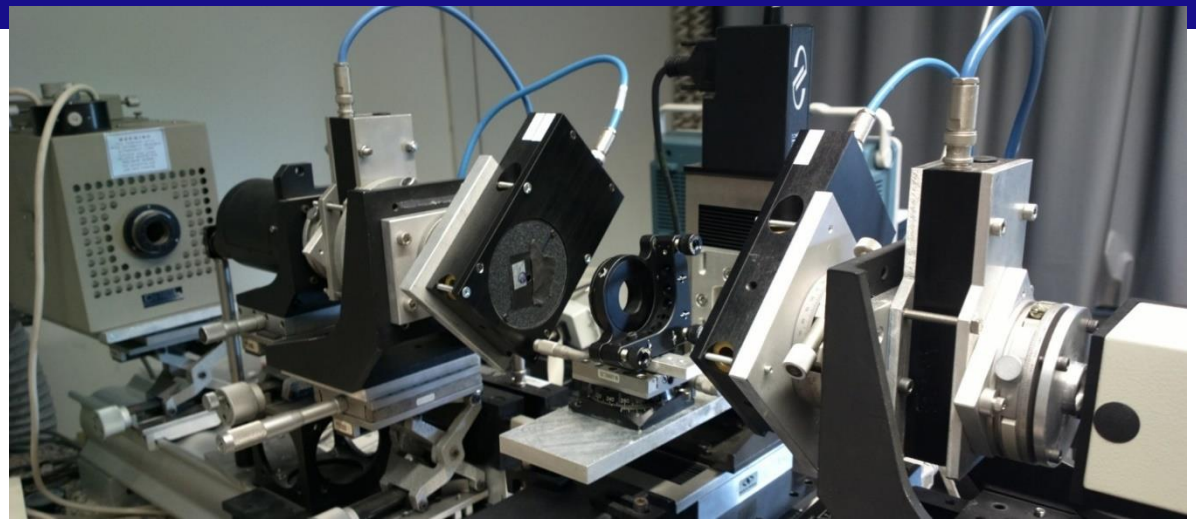

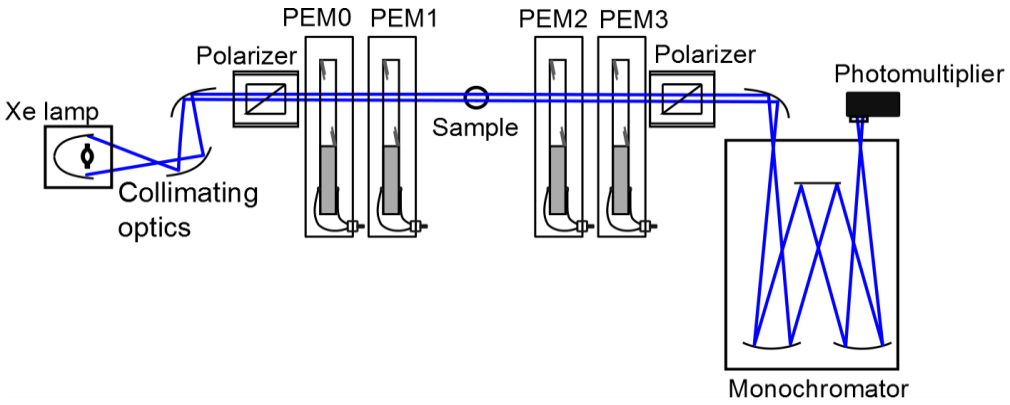

$$\mathbf{S_{out}} = \mathbf{P_1}\mathbf{M}^{0^o}_{PEM\,3}\mathbf{M}^{45^o}_{PEM\,2}\mathbf{M}_{sample}\mathbf{M}^{45^o}_{PEM\,1}\mathbf{M}^{0^o}_{PEM\,0}\mathbf{P_0}\mathbf{S_{in}}$$

$$I_n = \begin{pmatrix} 1 & X_2X_3 & -Y_3 & X_3Y_2 \end{pmatrix} \begin{bmatrix} m_{00} & m_{01} & m_{02} & m_{03} \\ m_{10} & m_{11} & m_{12} & m_{13} \\ m_{20} & m_{21} & m_{22} & m_{23} \\ m_{30} & m_{31} & m_{32} & m_{33} \end{bmatrix} \begin{bmatrix} 1 \\ X_0X_1 \\ -Y_0 \\ X_0Y_1 \end{bmatrix}$$

$$X_i = \cos(\delta_i) = \cos(A\sin(\omega t + \phi))$$

$$Y_i = \sin(\delta_i) = \sin(A\sin(\omega t + \phi))$$

O. Arteaga, J. Freudenthal, B. Wang, and B. Kahr, "Mueller matrix polarimetry with four photoelastic modulators: theory and calibration," Appl. Opt. 51, 6805-6817 (2012)

3. Optimizing a 4-photoelastic modulator MM ellipsometer

For **almost ten years we have been using a non-optimal acquisition** caused by the “common” approach of expressing the detected intensity in Fourier components

For this system the complete Fourier expansion includes an infinite number of harmonics

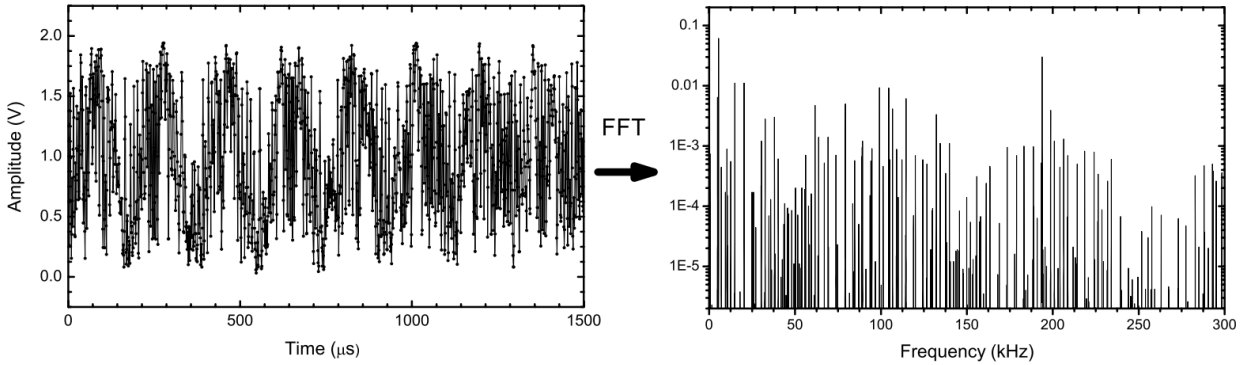

$$X_i = \cos(\delta_i) = \cos(A\sin(\omega t + \phi)) = 2\sum_{k=1}^{\infty} J_{2k-1}(A)\sin[(2k-1)(\omega t + \phi)]$$

$$Y_i = \sin(\delta_i) = \sin(A\sin(\omega t + \phi)) = J_0(A) + 2\sum_{k=1}^{\infty} J_{2k}\cos[2k(\omega t + \phi)]$$

Mueller matrix determination was based on a subset (16) of harmonics

Avoid the Fourier analysis!

$$\mathbf{I} = \mathbf{W}\vec{\mathbf{M}}$$

$$\vec{\mathbf{M}} = \mathbf{W}^{+}\mathbf{I}$$

$$\mathbf{W}^{+} = (\mathbf{W}^{T}\mathbf{W})^{-1}\mathbf{W}^{T}$$

The elements of **W** do not need any particular form and it is always the *best* solution

3. Optimizing a 4-photoelastic modulator MM ellipsometer

Simulations

Fixed sampling (500 kHz) varying # of intensities

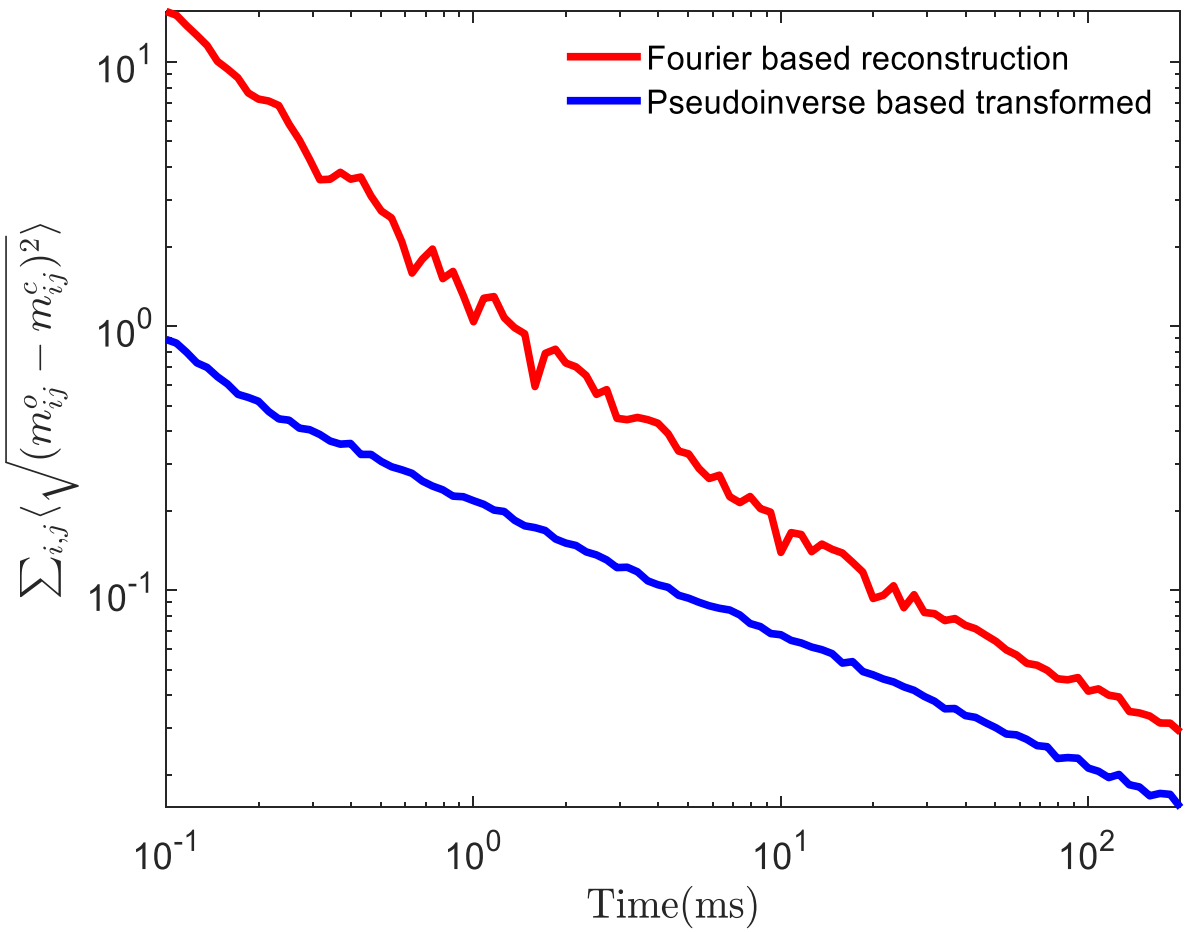

Fixed # of intensities (100000) varying sampling frequency

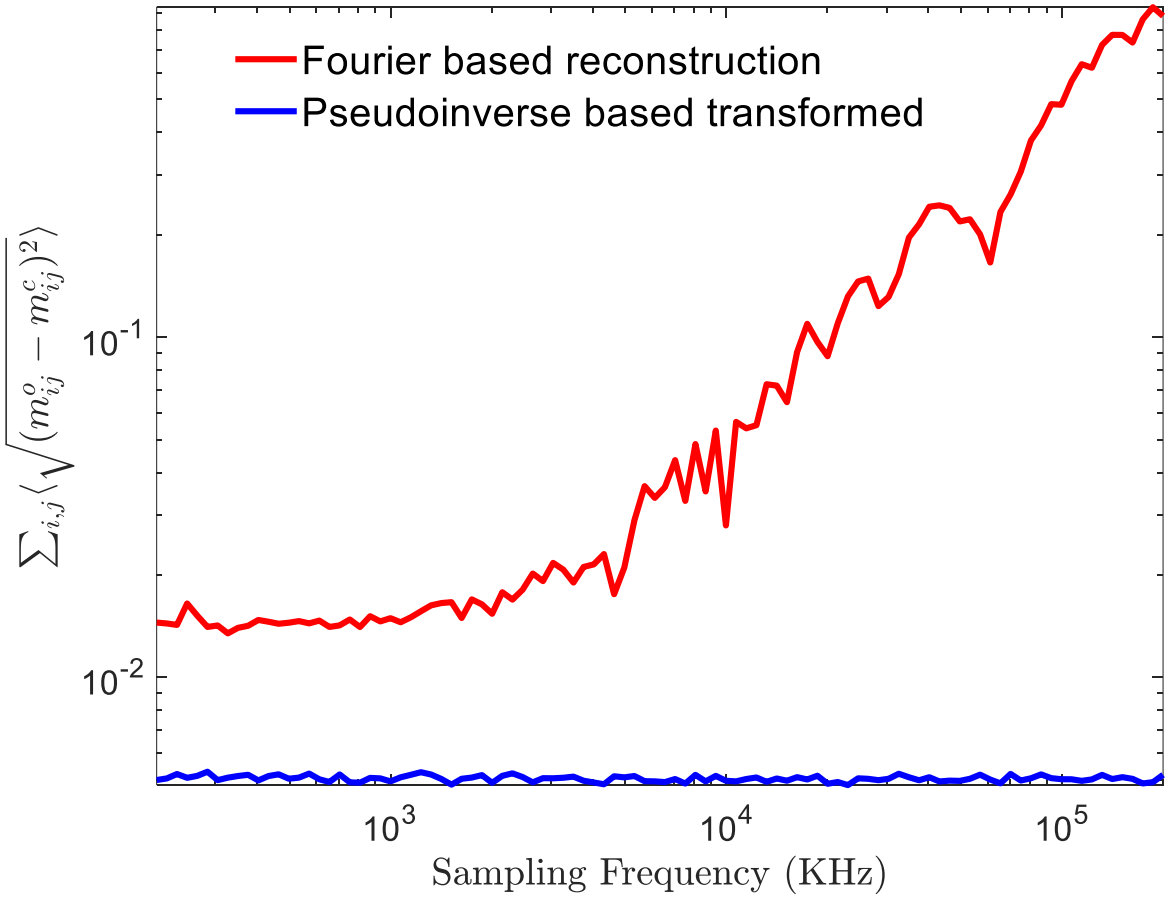

3. Optimizing a 4-photoelastic modulator MM ellipsometer

Standard deviations (x500) after 5 averages (experimental) in transmission (air sample)

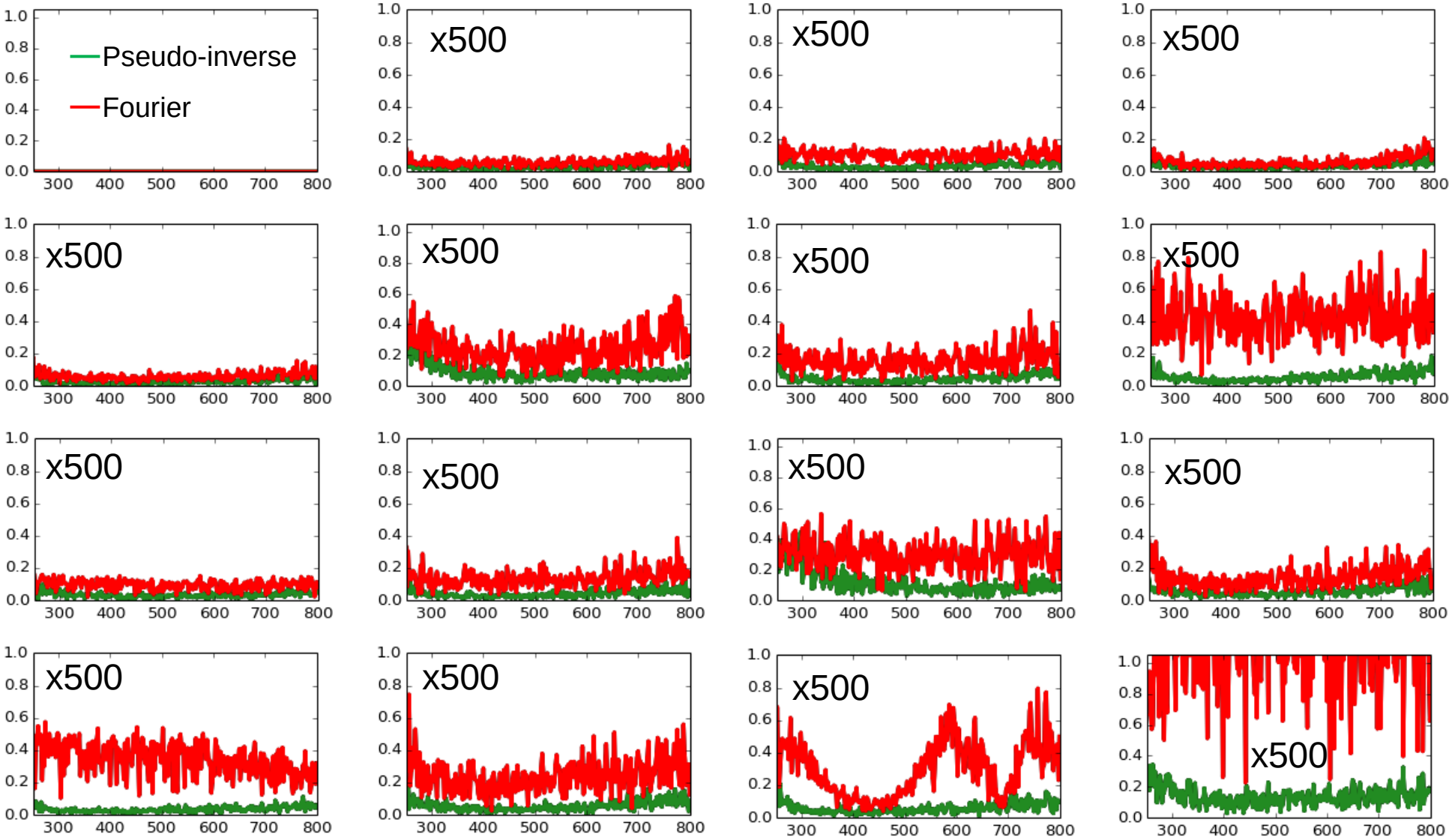

4. Spatial dispersion

Spatial dispersion is the non-local dependence of material parameters (the response to the field occurs over a neighborhood of the point where the field is applied)

Origin: Finite wave vector of light, $\vec{k}$, which breaks symmetry of light-matter interaction

Expansion in powers of k

$$\varepsilon_{ij}(\omega,\vec{k}) = \varepsilon_{ij}(\omega) + i\gamma_{ijk}(\omega)k_k + \alpha_{ijkl}(\omega)k_k k_l$$

$$\varepsilon_{ij}^{-1}(\omega,\vec{k}) = \varepsilon_{ij}^{-1}(\omega) + i\delta_{ijk}(\omega)k_k + \beta_{ijkl}(\omega)k_k k_l$$

First order term

Optical activity (consequence of spatial dispersion). e.g. to "see" the handedness of a structure the finite wavelength of light or wavevector must be accounted

$$\sim \frac{a}{\lambda}$$

Second-order term

Usually, this is the term called *spatial dispersion*.

$$\sim \left(\frac{a}{\lambda}\right)^2$$

In natural materials, spatial dispersion can be only observed as a weak effect

$$\frac{a}{\lambda} \ll 1$$

In metamaterials it can be a large effect

4. Spatial dispersion

Experimental History

H. A. Lorentz prediction of the effect in 1879 and an "unclear" experiment in NCl (1921) ***Transmission***

Physics. — *"Double refraction by regular crystals"*. By Prof. H. A. LORENTZ.

(Communicated at the meeting of November 26, 1921).

First clear experimental demonstrations by Pastrnak and Vedam in Si and by Cardona and Yu in GaAs (1971) ***Transmission***

Optical Anisotropy of Silicon Single Crystals*

J. Pastrnak† and K. Vedam‡

Materials Research Laboratory, The Pennsylvania State University, University Park, Pennsylvania 16802

(Received 21 September 1970)

The birefringence of Si single crystal was measured for He-Ne laser light of wavelength $\lambda = 1.15\ \mu$ propagating along ⟨110⟩ directions, and found to be $\Delta n = n_{\langle 110\rangle} - n_{\langle 100\rangle} = (5.04 \pm 0.12)$

Above Band-Gap measurements by Aspnes and colleagues (1980's and 1990's) ***Normal incidence reflection***

Anisotropies in the Above–Band-Gap Optical Spectra of Cubic Semiconductors

D. E. Aspnes and A. A. Studna

Bell Communications Research, Inc., Murray Hill, New Jersey 07974

(Received 24 August 1984; revised manuscript received 1 March 1985)

We report the first systematic study of above–band-gap optical anisotropies in cubic semiconductors. The anisotropies are large, of the order of 1%. The dominant intrinsic contributions for (110)

Implications of spatial dispersion in UV optics. 193nm and 157 nm lithography (early 2000's) ***Transmission***

Intrinsic birefringence in calcium fluoride and barium fluoride

John H. Burnett, Zachary H. Levine, and Eric L. Shirley

National Institute of Standards and Technology, Gaithersburg, Maryland 20899

(Received 14 May 2001; revised manuscript received 26 September 2001; published 29 November 2001)

We report measurements of the intrinsic birefringence in CaF_2 and BaF_2 for wavelengths in the range 365

4. Spatial dispersion

Cubic crystals (classes m3m or O_h) symmetry

$$\varepsilon_{ij}(\omega,\vec{k}) = \varepsilon_{ij}(\omega) + i\gamma_{ijk}(\omega)k_k + \alpha_{ijkl}(\omega)k_k k_l$$

$$\varepsilon_{ij}^{-1}(\omega,\vec{k}) = \varepsilon_{ij}^{-1}(\omega) + i\delta_{ijk}(\omega)k_k + \beta_{ijkl}(\omega)k_k k_l$$

$$\Rightarrow$$

$$\varepsilon_{ij}(\omega,\vec{k}) = \varepsilon_{ij}(\omega) + \alpha_{ijkl}(\omega)k_k k_l$$

$$\varepsilon_{ij}^{-1}(\omega,\vec{k}) = \varepsilon_{ij}^{-1}(\omega) + \beta_{ijkl}(\omega)k_k k_l$$

Expressed as a 6x6 matrix:

$$\alpha_{ij} = \begin{pmatrix} \alpha_{11} & \alpha_{12} & \alpha_{12} & 0 & 0 & 0 \\ \alpha_{12} & \alpha_{11} & \alpha_{12} & 0 & 0 & 0 \\ \alpha_{12} & \alpha_{12} & \alpha_{11} & 0 & 0 & 0 \\ 0 & 0 & 0 & \alpha_{44} & 0 & 0 \\ 0 & 0 & 0 & 0 & \alpha_{44} & 0 \\ 0 & 0 & 0 & 0 & 0 & \alpha_{44} \end{pmatrix}$$

(same form as piezo-optic tensor)

Both for transmission and reflection measurements, only the linear combination can be measured

$$p = \alpha_{11} - \alpha_{12} - 2\alpha_{44}$$

4. Spatial dispersion

For silicon or other diamond cubic materials

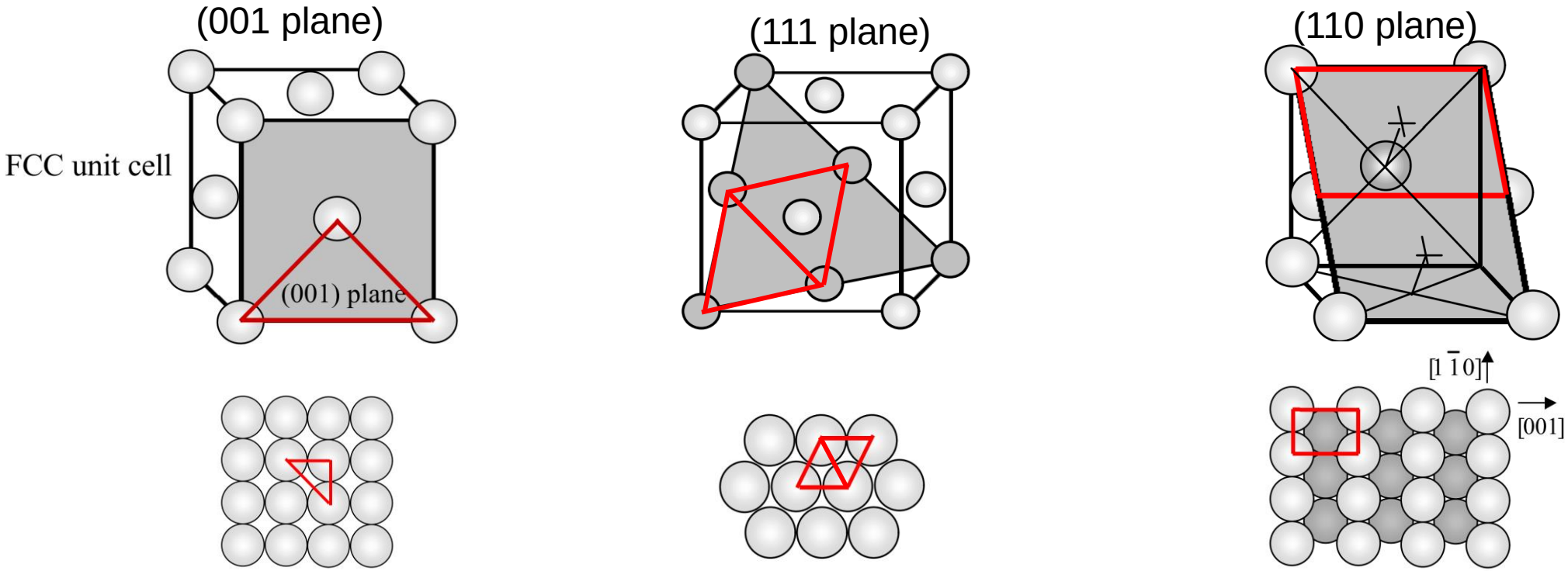

Transmission	No anisotropy for $\vec{k} \parallel \langle 001 \rangle$ or $\vec{k} \parallel \langle 111 \rangle$	Anisotropy for $\vec{k} \parallel \langle 110 \rangle$
Reflection	Extremely weak or no cross-polarization for 001 and 111 wafers	Cross-polarization depending on the azimuth for 110 wafers

4. Spatial dispersion

Transmission on a 110 silicon wafer (dual rotating compensator)

$$(\mathbf{M}-\mathbf{I})\times 10$$

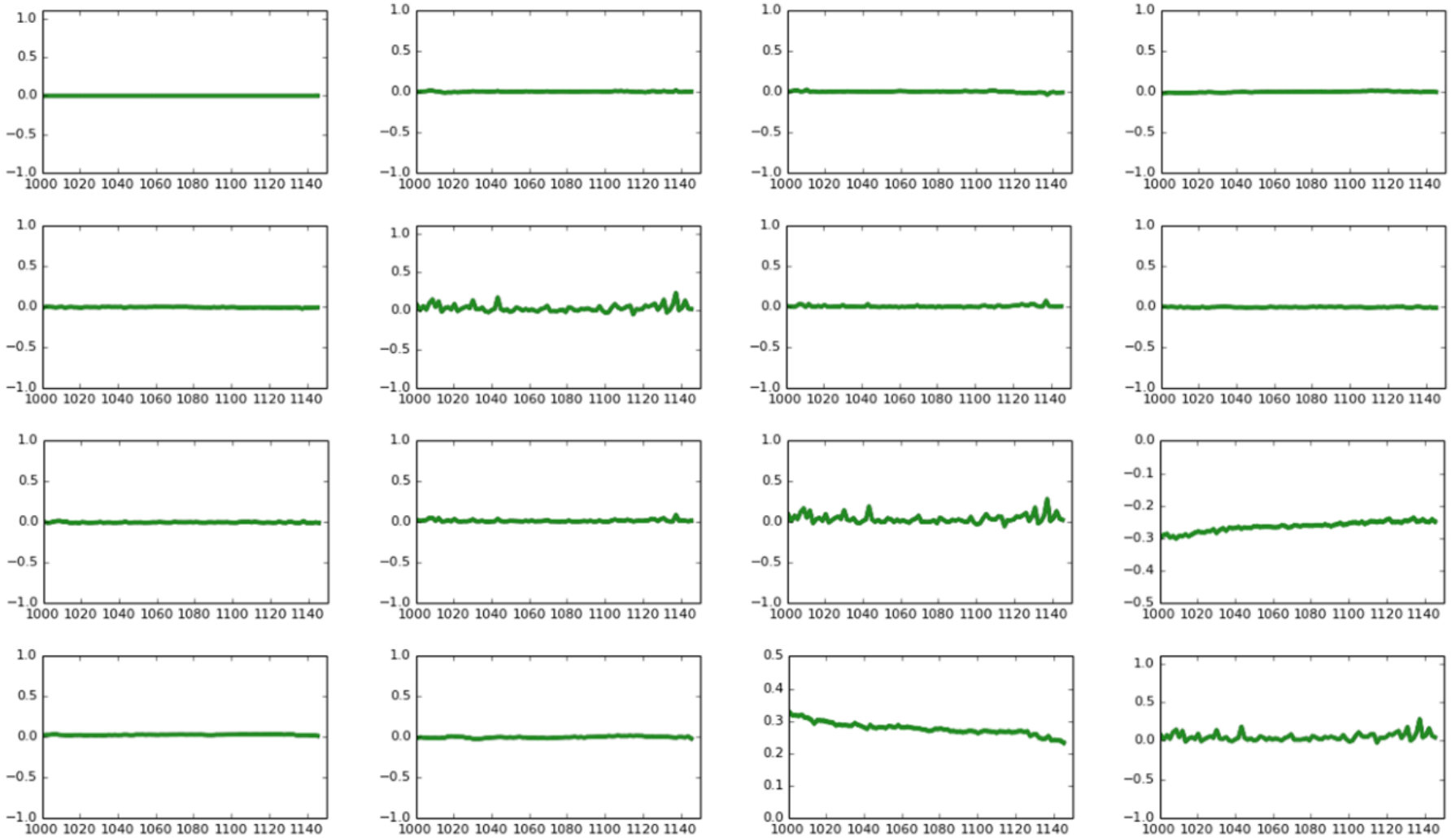

4. Spatial dispersion

Transmission 110 silicon wafer (dual rotating compensator)

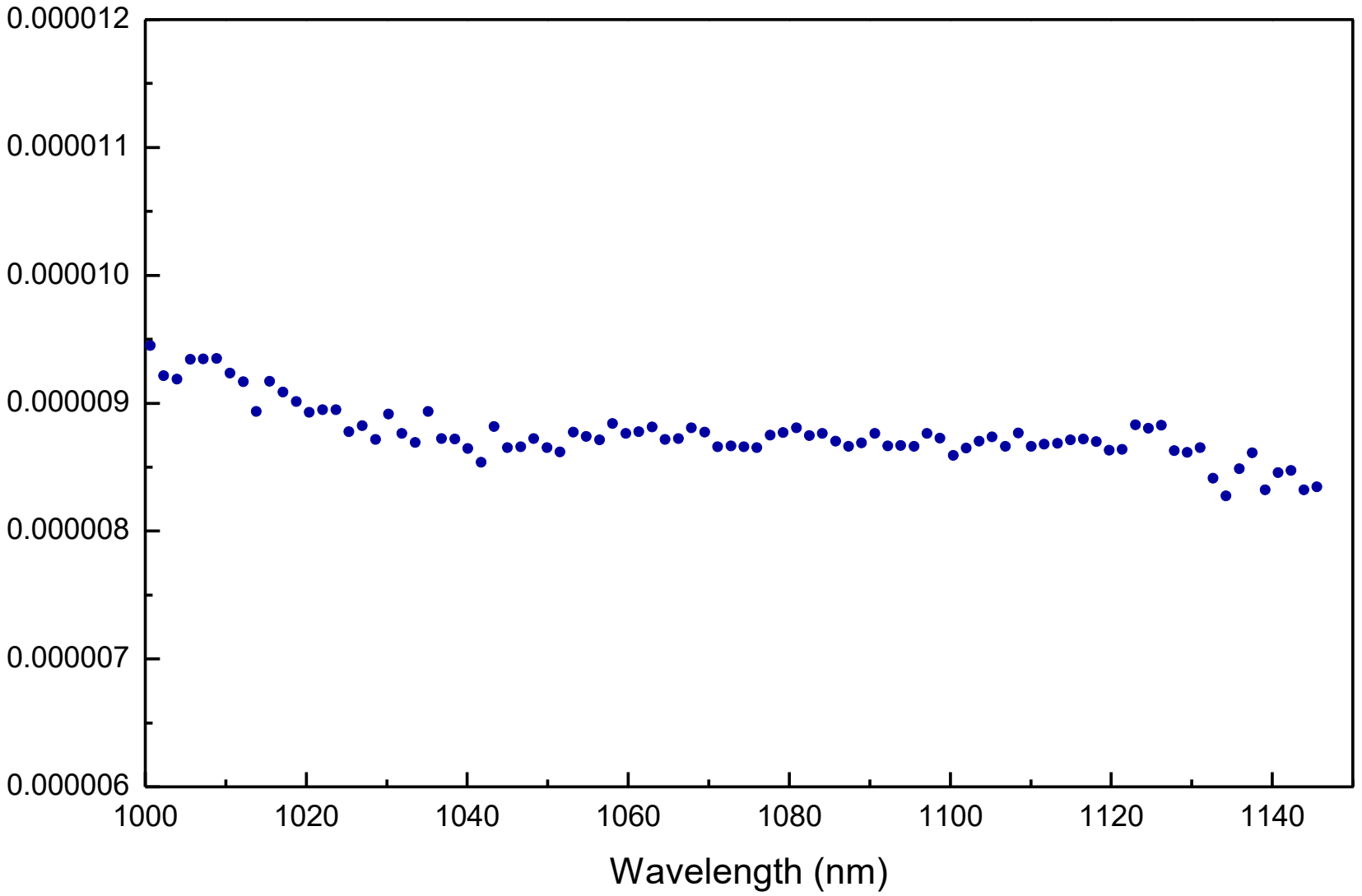

$$\Delta n \simeq (8.7 \pm 0.2) \times 10^{-6}$$

$$\lambda = 1050 \text{ nm}$$

The anisotropy is larger above the band gap

4. Spatial dispersion

4-PEM 110 Si

45º
135º
0º
90º

Angles of wafer flat (001) direction with respect to the perpendicular to the plane of incidence

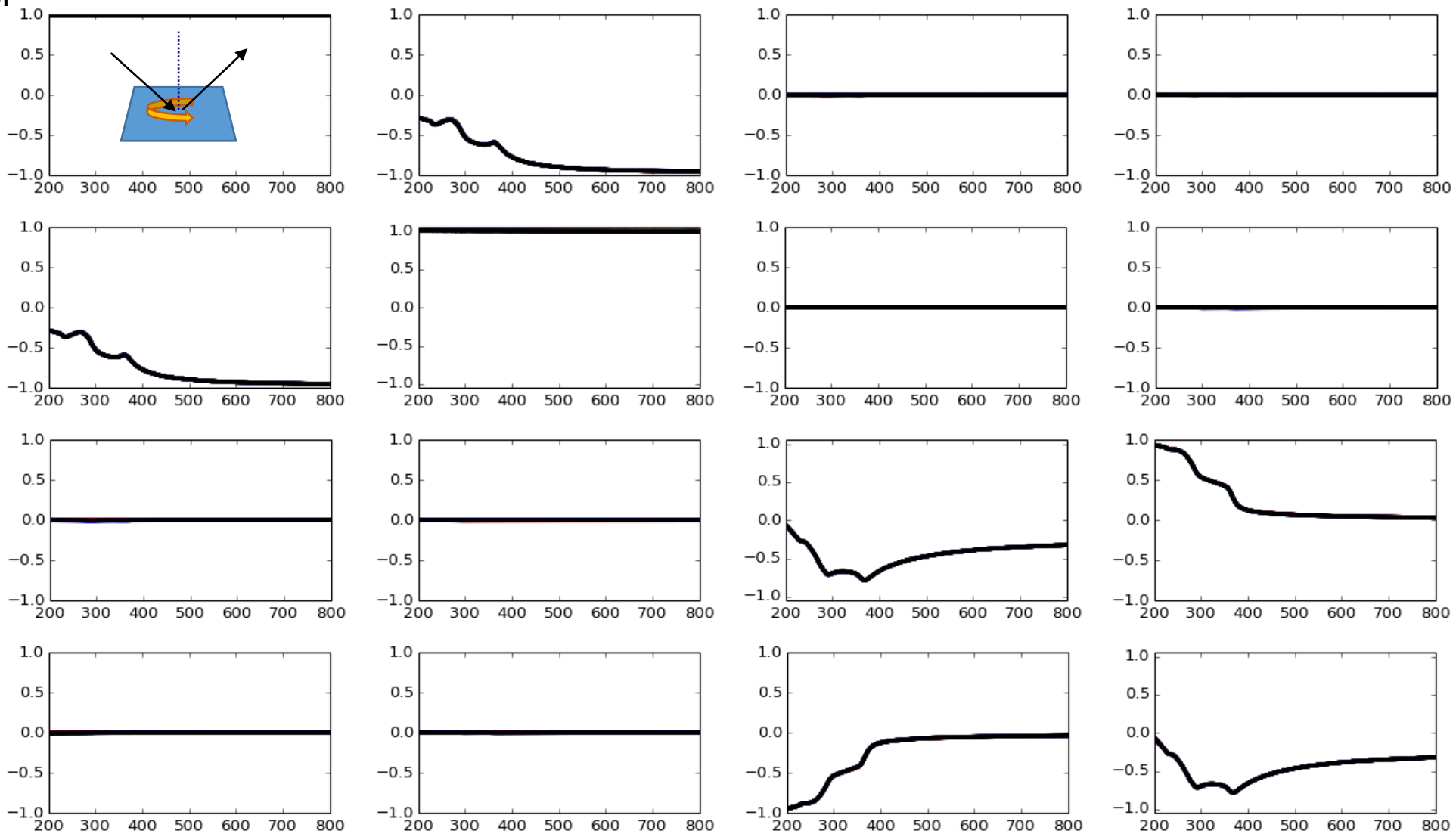

4. Spatial dispersion

4-PEM 110 Si

45º
135º
0º
90º

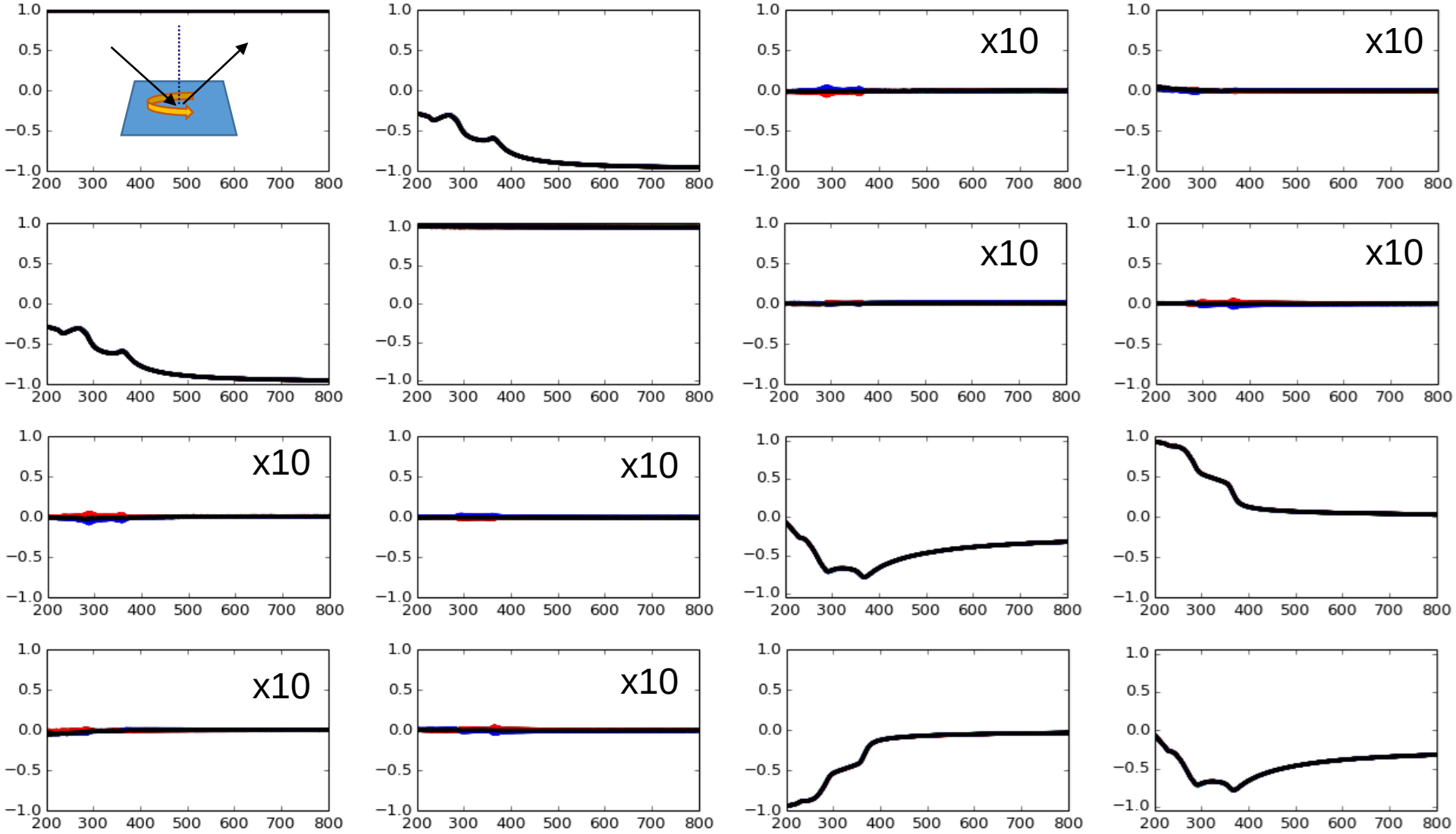

4. Spatial dispersion

4-PEM 110 Si

45º
135º
0º
90º

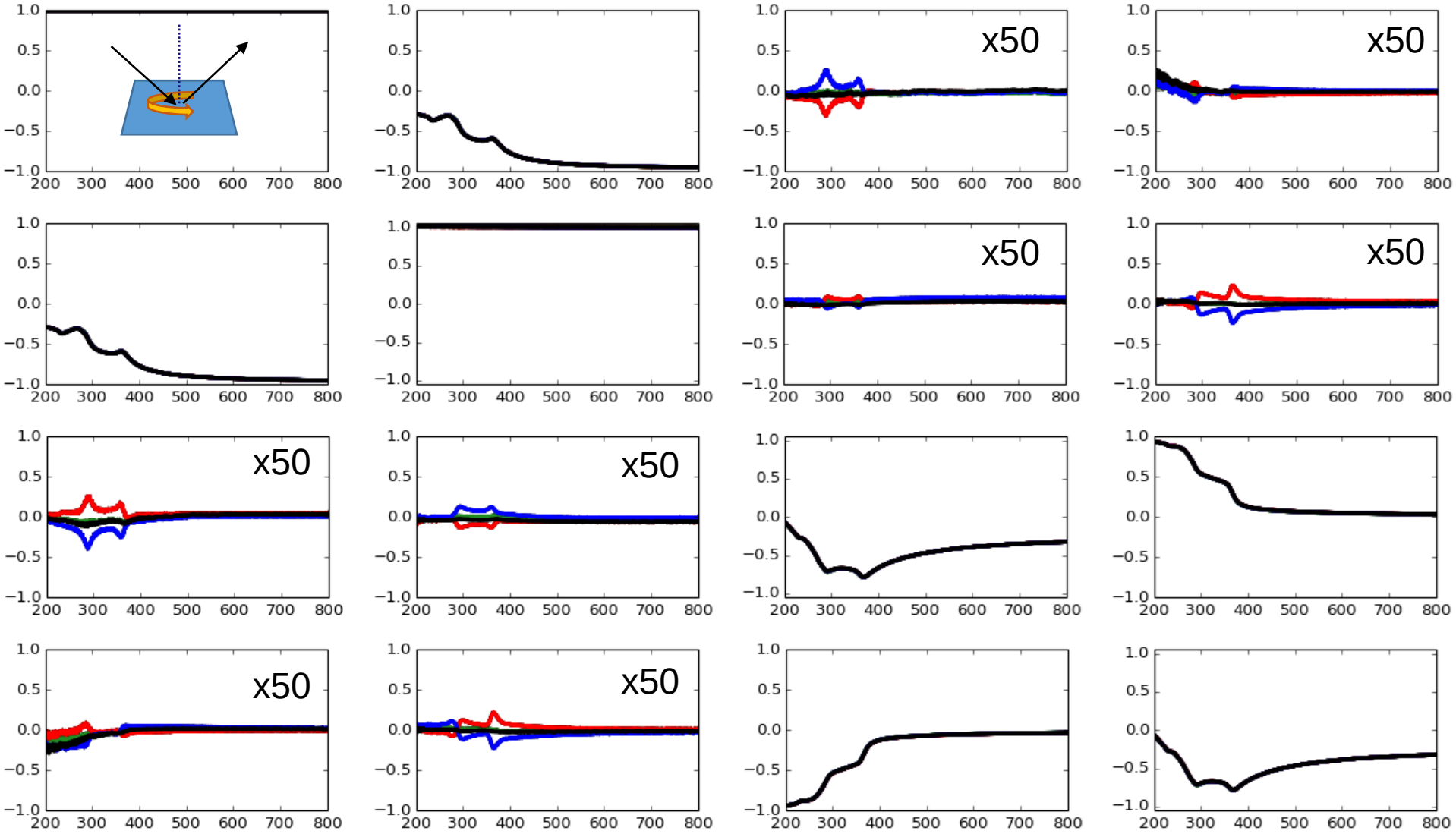

4. Spatial dispersion

4-PEM 110 Si

45º
135º
0º
90º

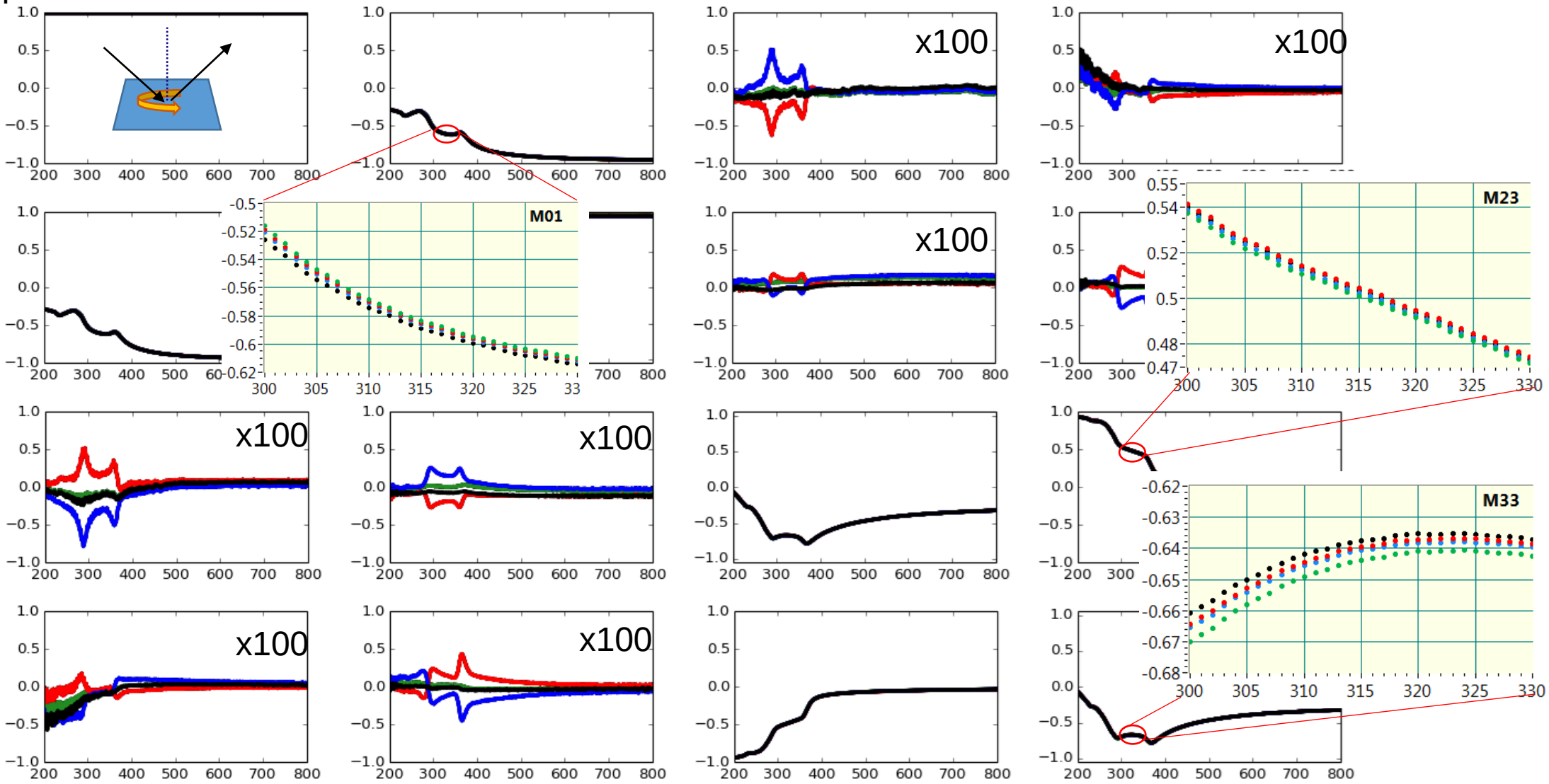

4.Spatial dispersion

Dual-rotating compensator 110 Si

45º
135º
0º
90º

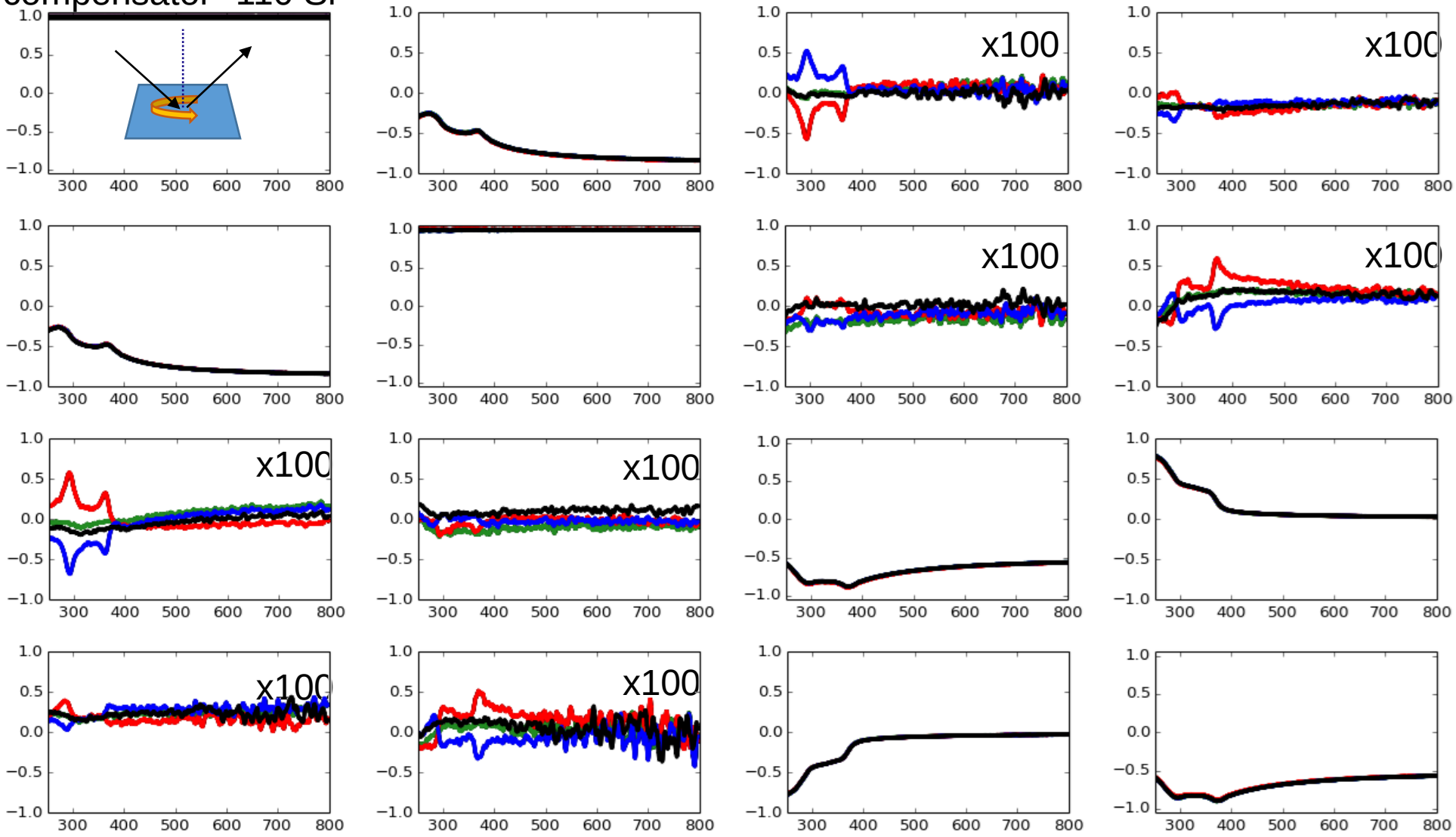

4. Spatial dispersion

4PEM 001 Si

45º
135º
0º
90º

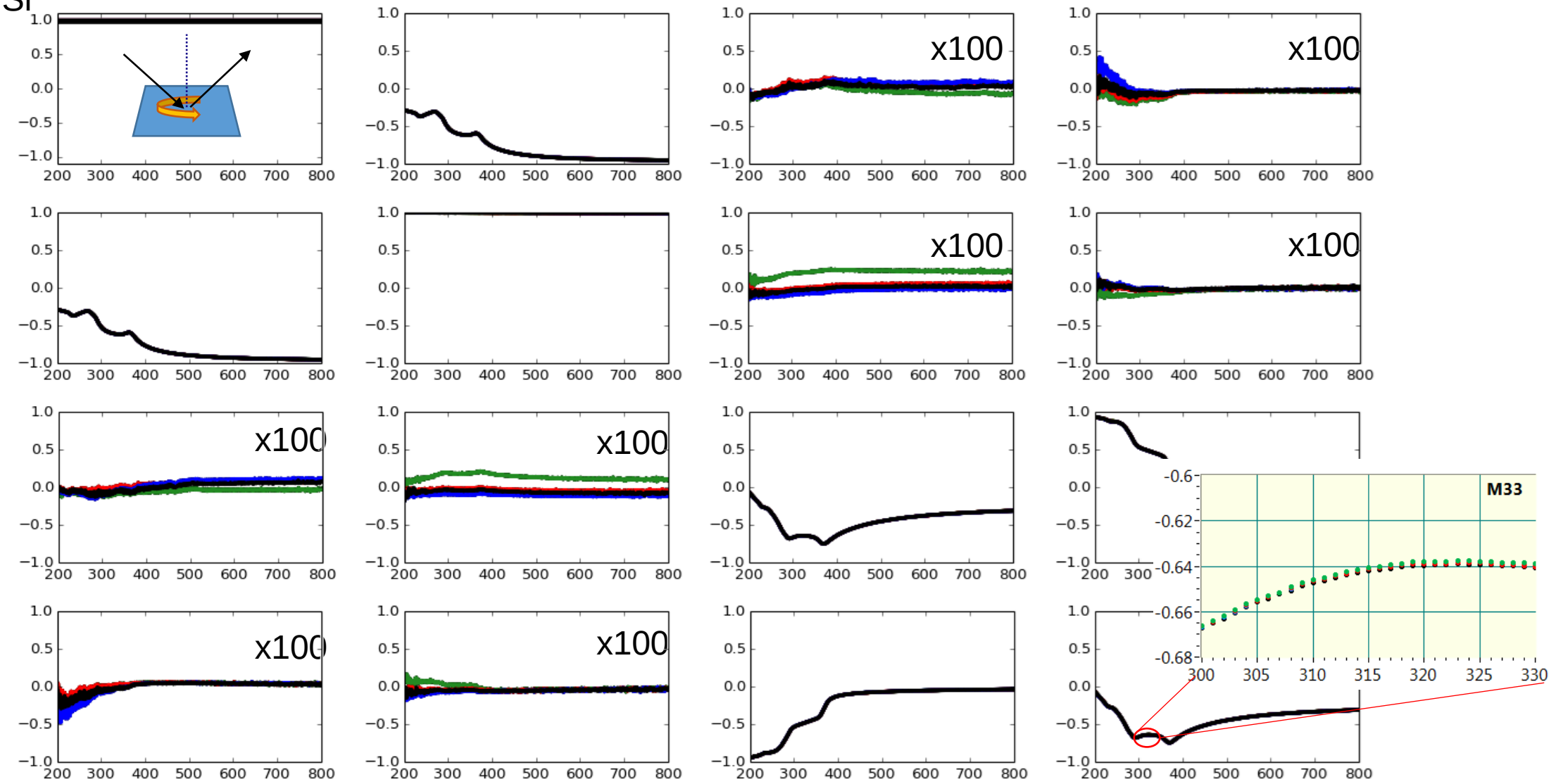

4. Spatial dispersion

Wavelength-by-wavelength fit with Berreman's 4x4 matrix transfer formalism

- Experimental data: 4 Mueller matrix datasets between 200 nm - 800nm at different azimuths
- Determined Parameters (at each wavelength) : $\mathrm{Re}(\varepsilon)$, $\mathrm{Im}(\varepsilon)$, $\mathrm{Re}(p)$, $\mathrm{Im}(p)$
- SiO_2 Overlayer: fixed at 2.52nm from a previous combined fit (disregarding SD)
- AOI: 70.02º

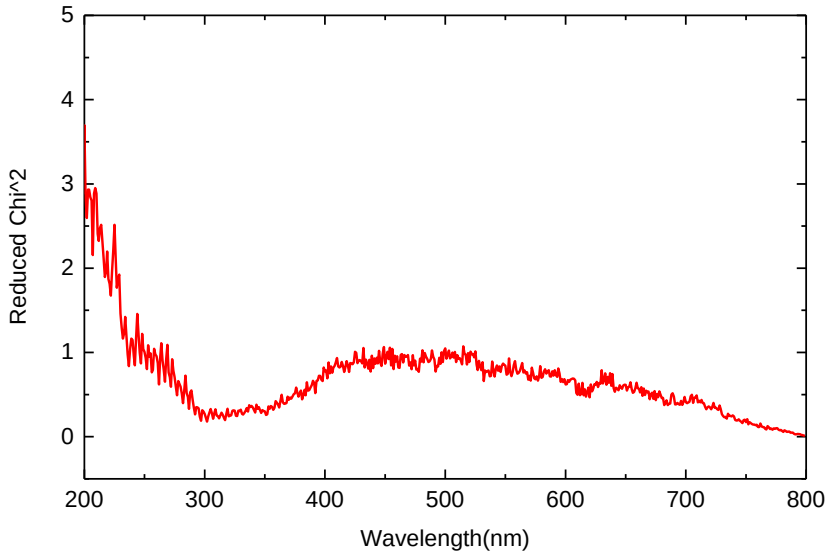

4. Spatial dispersion

Dielectric constant ε

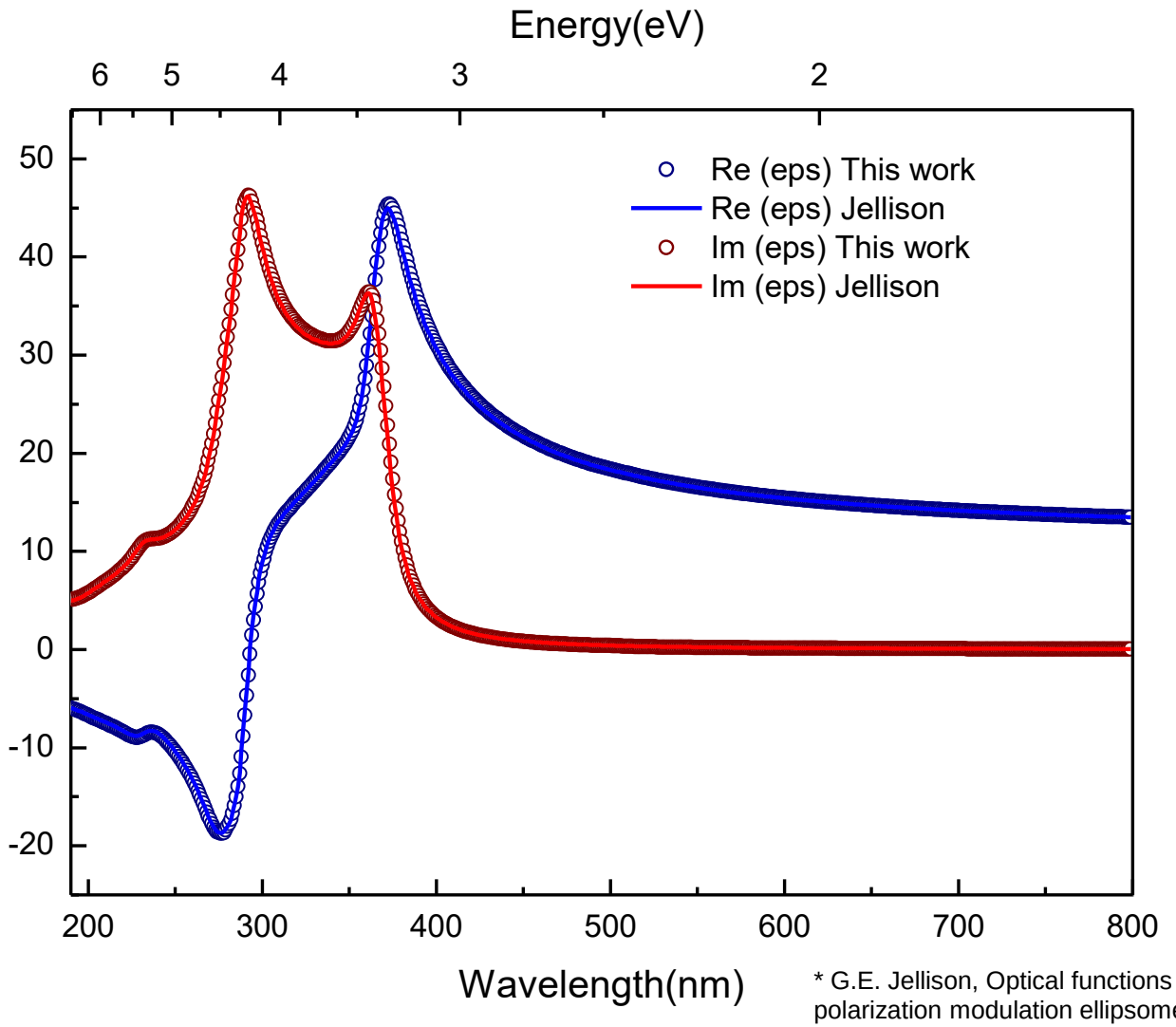

Spatial dispersion p

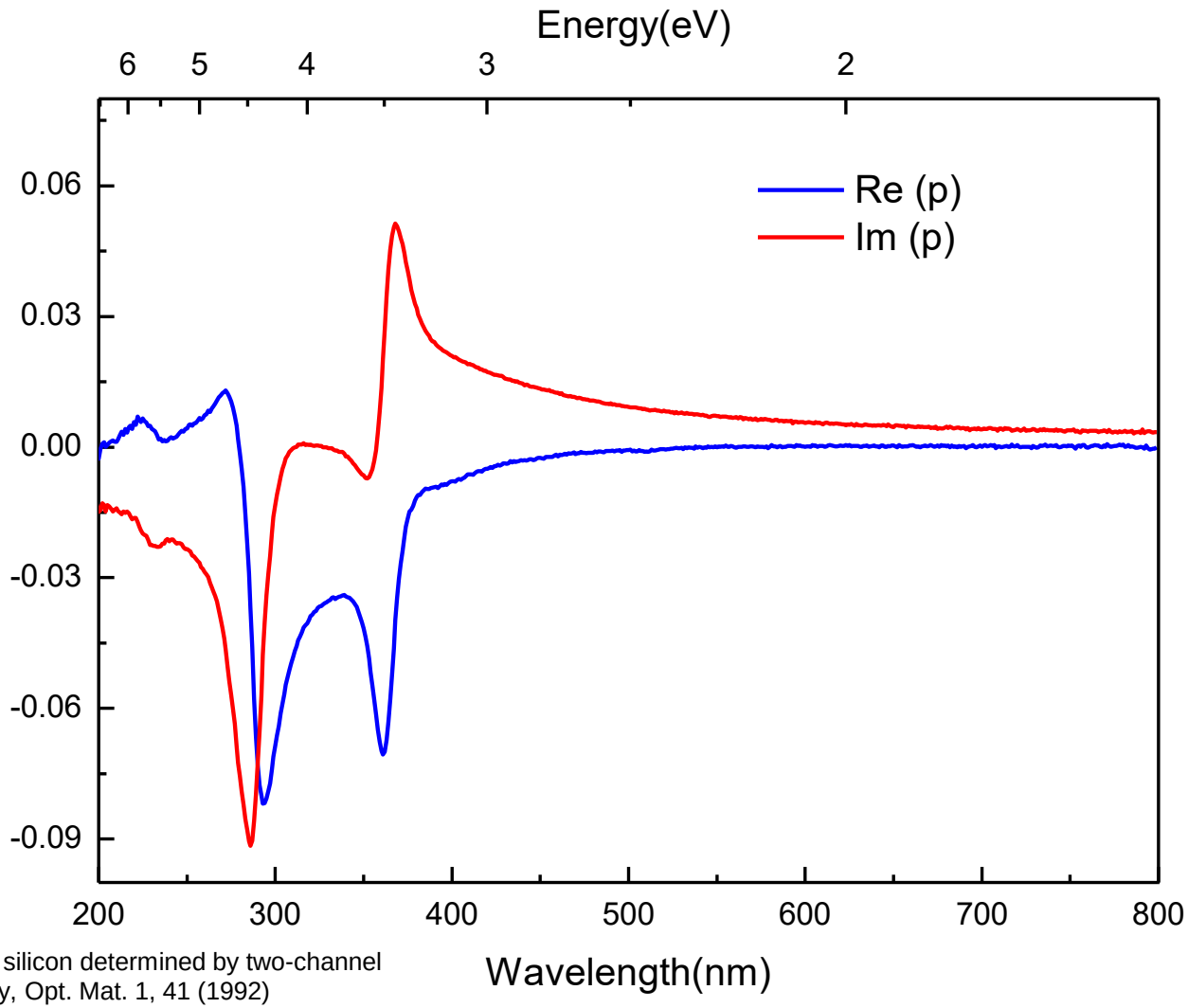

* G.E. Jellison, Optical functions of silicon determined by two-channel polarization modulation ellipsometry, Opt. Mat. 1, 41 (1992)

4. Spatial dispersion

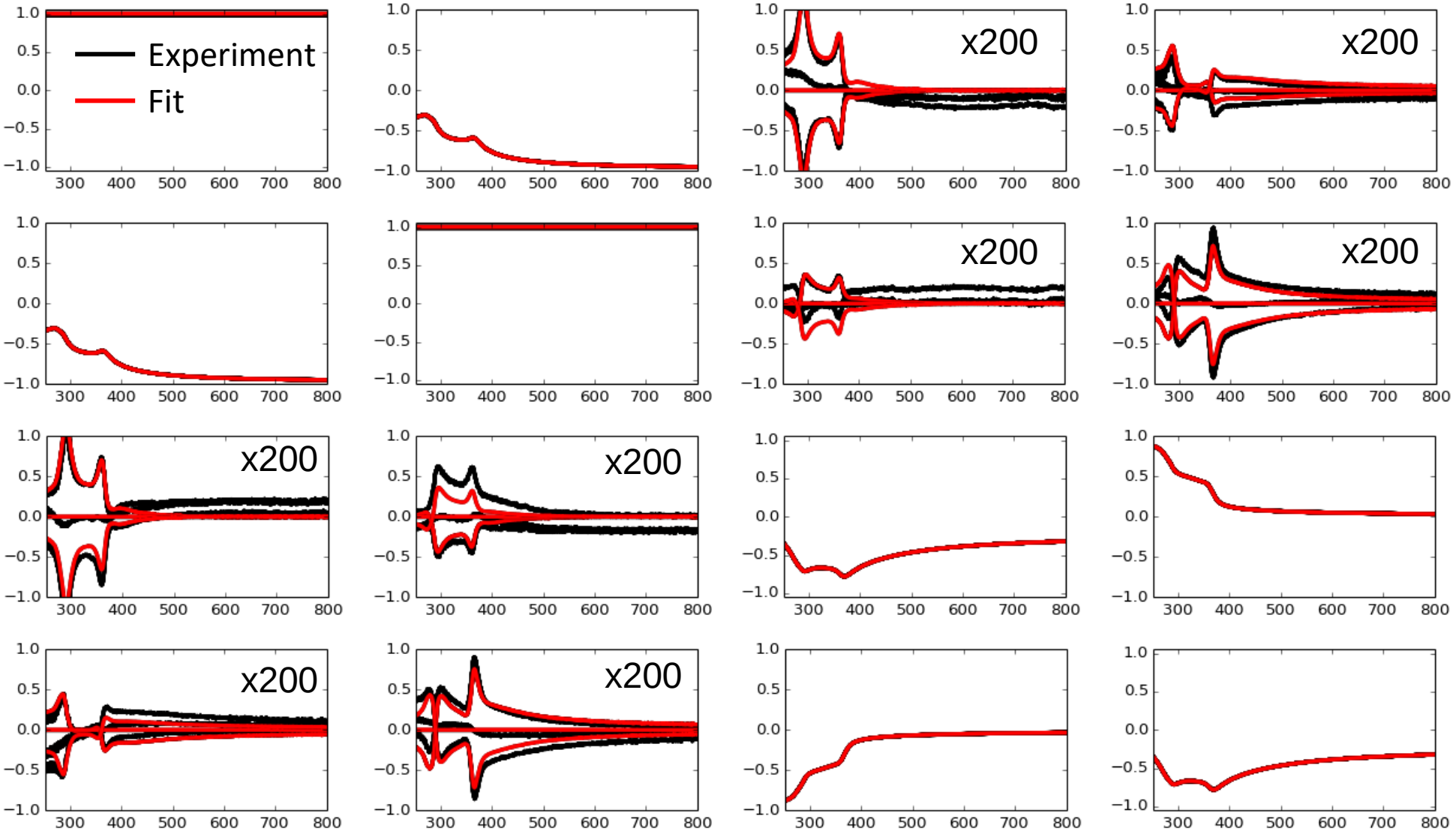

Proposal(a challenging measurement)

Using (110) Si wafers to assess the performance of MM ellipsometers (instrument's sensitivity + mechanical accuracy in the orientation)

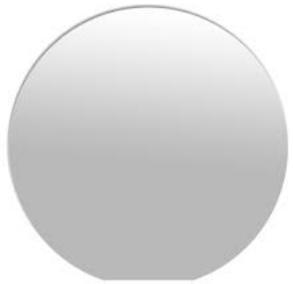

Acknowledgements

Razvigor Ossikovski

Subiao Bian

Adolf Canillas

Jordi Gomis-Brescó

Esther Pascual

Thank you for your attention!